Basic principles in starch multi-scale structuration to mitigate digestibility: A review

Chengdeng Chi, Xiaoxi Li, Shuangxia Huang, Ling Chen, Yiping Zhang, Lin Li, Song Miao

PII: S0924-2244(21)00024-8

DOI: https://doi.org/10.1016/j.tifs.2021.01.024

Reference: TIFS 3102

To appear in: *Trends in Food Science & Technology*

Received Date: 17 May 2020

Revised Date: 6 January 2021

Accepted Date: 7 January 2021

Please cite this article as: Chi, C., Li, X., Huang, S., Chen, L., Zhang, Y., Li, L., Miao, S., Basic principles in starch multi-scale structuration to mitigate digestibility: A review, *Trends in Food Science & Technology* (2021), doi: https://doi.org/10.1016/j.tifs.2021.01.024.

Basic principles in starch multi-scale structuration to mitigate digestibility: A review

Chengdeng Chi [a], Xiaoxi Li [a, *], Shuangxia Huang [a], Ling Chen [a], Yiping Zhang [a], Lin Li [a], Song Miao [b, *]

[a] Ministry of Education Engineering Research Center of Starch and Protein Processing, Guangdong Province Key Laboratory for Green Processing of Natural Products and Product Safety, School of Food Science and Engineering, South China University of Technology, Guangzhou 510640, China

[b] Teagasc Food Research Centre, Moorepark, Fermoy, Co. Cork P61 C996, Ireland

[*] **Correspondence:** Xiaoxi Li and Song Miao

E-mail: xxlee@scut.edu.cn (X. Li) or song.miao@teagasc.ie (S. Miao)

ABSTRACT

Background: In the human diet, starch makes a significant contribution to the maintenance of human nutrition and health due to its controlled digestibility. Starch digestion is controlled by its microstructure. Increasing developments in the modification of starch multi-scale structures that modulate digestibility have taken place due to increasing attention to health-promoting starchy foods. The process of starch structuration is a challenging concern in food science since the basic principles for designing starch structures with a specific digestibility are unknown.

Scope and Approach: Starch multi-scale structures significantly affect digestibility. However, starch digestibility cannot be precisely modulated without a solid theory of starch structuration to inform the tailoring of the digestibility of starchy foods. In this review, the effects of starch multi-scale structures (fine structures of amylose and amylopectin; short-range ordered structures; helical, crystalline, lamellar, aggregate structures; and structures formed after food processing) on the digestibility and the molecular mechanisms of the regulation of starch digestion are comprehensively discussed. The key structures that can be manipulated for target-modulation of starch digestibility are summarized.

Key Findings and Conclusions: Basic principles for mitigating starch digestibility, such as increasing the thickness of semi-crystalline lamellae and crystalline lamellae, nanoscale aggregates, V-, A-, or B-type crystals, double helices, long amylopectin helices, short-range ordered structures, the content of amylose fractions and

high-branched amylopectin are established. Ordered starch structures, including short-range and long-range ordered structures, play critical roles in mitigating starch digestibility while faulty- and perfectly arranged helical, crystalline, lamellar structures, and nano aggregates are proposed to be slowly digestible and resistant starches, respectively.

Keywords

Starch digestibility; multi-scale structures; slowly digestible starch; resistant starch; structuration

1. Introduction

Starch is one of the most important polysaccharide macronutrients and is normally processed before consumption in the human diet (Svihus & Hervik, 2016). Processed starch (cooked, steamed, baked, and fried starch) with specific digestibility plays an important role in human nutrition (Chen et al., 2019; Selma-Gracia, Laparra, & Haros, 2020; Wang et al., 2020). It is accepted that starch digestion starts in the mouth and mainly occurs in the small intestine where pancreatic α-amylase, dextrinase, amyloglucosidase, α-glucosidase, and maltase are embedded. Based on the extent and rate of starch digestion, starch can be classified into rapidly digestible starch (RDS), slowly digestible starch (SDS), and resistant starch (RS) (Englyst, Kingman, & Cummings, 1992). RDS increases human blood glucose levels immediately after starch ingestion, providing necessary energy for the human body and maintaining normal physiological functions of the human brain and central nervous system (Englyst et al., 1992; Svihus et al., 2016; Vaclavik & Christian, 2014). Glucose freed from the digestion of RDS-enriched foods contributes to a rapid increase in the human postprandial blood glucose concentration and a high glycemic response, which can induce diet-related metabolic chronic diseases such as type II diabetes mellitus (Brennan, 2005). SDS is digested slowly but completely in the small intestine to maintain a stable glucose concentration in the human blood stream (Englyst et al., 1992; Miao, Jiang, Cui, Zhang, & Jin, 2015a; Zhang & Hamaker,

2009). RS cannot be digested in the human upper gastrointestinal tract but is degraded by microflora in the colon through anaerobic fermentation (Englyst et al., 1992), which is a benefit to the regulation of gut microbiota and the prevention of metabolic diseases (Bindels, Walter, & Ramer-Tait, 2015; Duan et al., 2019; Rehman et al., 2012).

Essentially, starch digestion is controlled by the starch microstructure. The microstructure of starch is complex and organized in multiple scales. Starch multi-scale structures, including the amylose/amylopectin ratio, fine structures of amylose and amylopectin, short-range ordered structures, helical structures, crystalline features, lamellar structures, and morphology, are factors that determine enzyme binding and catalyzation with starch in the human diet (Pu, Chen, Li, & Li, 2013; Xu et al., 2019). Non-starchy ingredients in foods such as protein, polysaccharides, lipids, and cell walls complex with starch molecules and change starch multi-scale structures, causing significant suppression of enzymes accessibility to starch molecules(Chen et al., 2018; Rovalino-Córdova, Fogliano, & Capuano, 2018; Wu, He, Hong, & Wang, 2016; Ye et al., 2018; Yu et al., 2018). Furthermore, food processing alters starch structures to form new multi-scale structures, influencing the digestibility of processed starch. Depending on processing conditions such as heat-moisture treatment and annealing (Trung, Ngoc, Hoa, Tien, & Hung, 2017; Yan, Feng, Shi, Cui, & Liu, 2020; Yang et al., 2019), hydrothermal-cooling (Selma-Gracia

et al., 2020; Wang, Wang, Liu, Wang, & Copeland, 2017), cooking (Martinez et al., 2018; Tester, Qi, & Karkalas, 2006; Wang et al., 2020), baking (Chen et al., 2019; Gao et al., 2021), frying (Contardo, James, & Bouchon, 2020; Li et al., 2020; Yang et al., 2020), and enzymatic debranching (Chen, Li, Shih, & Pai, 2020; Li, Zhang, Xie, & Chen, 2019), starch multi-scale structures change and form new hierarchical structures. Different degrees of starch digestion with different SDS and/or RS contents are then obtained (Dupuis, Liu, & Yada, 2014; Miao et al., 2015a; Zhang et al., 2009). Importantly, the starch structures of ready-to-eat processed starchy foods ultimately determine starch digestion. Studies have summarized the links between the ratio of amylose to amylopectin, starch crystalline structures, granular features with the digestibility (Magallanes, Flores, & Bello, 2017; Tian et al., 2018; Toutounji et al., 2019). The actions of amylose and amylopectin fine structures, short-range ordered structures, and helical and semi-crystalline parameters on starch digestibility have been extensively investigated but not comprehensively discussed. When subjected to different types of food processing, starch molecules disassemble and reassemble, causing the formation of new multi-scale structures that significantly affect starch digestion. However, how starch multi-scale structuration during food processing influences the digestibility of processed starch is yet to be determined. Furthermore, the intramolecular and intermolecular interactions among starch molecules or starch with non-starchy ingredients within foods systems significantly yields complicated

starch structures which consist of different interaction-dominated multi-scale starch fractions. Food researchers currently rely on traditional methods to modulate starch structures and their subsequent digestibility. However, starch digestibility cannot be precisely modulated without a solid theory toward starch structuration for tailoring the digestibility of starchy foods. This in turn stimulates interest in a comprehensive discussion of the basic principles of starch multi-scale structuration to modulate digestibility. Moreover, the key structures that suppress enzymatic digestion and the structural features of RDS, SDS, and RS are unknown and therefore cannot guide starch targeting-structuration for the design of starchy foods with specific digestibility. Therefore, we focused on the topic of establishing principles of starch structuration to regulate starch digestibility. With increased consumer and market attention on health-promoting foods, the structuration of the key multi-scale structures of starch offers an attractive alternative to the rational design of SDS- or RS-enriched starchy foods, allowing for the further development of solutions to the production of foods with desired health-promoting functionality.

2. Brief introduction of starch multi-scale structures

Starches are α-D-glucose-derived polymers with multi-scale structures, as is schematically shown in **Figure 1**. Starch is composed of two main components: slightly branched amylose and highly branched amylopectin (Wang, Vilaplana, Wu, Hasjim, & Gilbert, 2019). The amylopectin chain is usually classified into three types,

A-, B-, and C-type, according to the branching points and degree of polymerization (DP). The A-chains refer to “outer” chains with no branching points and DP 6–12. The B-chains include B_1, B_2, and B_3 chains that vary in their respective length and the number of clusters they span. Typical DP for B_1, B_2, and B_3 chains are 13–24 (1), 25–36 (2), and ≥ 37 (3), respectively (Zhu, 2018). The single C chain per molecule likewise carries other chains as branches but contains the sole reducing terminal residue.

Starch chains can self-assemble to form helical structures with suitable chain length and the minimum amylopectin DP to form the double helical structure, which is 10 (Gidley & Bulpin, 1987). The chains with DP 14–24 (Shi & Seib, 1992) or DP 12–22 (Vandeputte, Vermeylen, Geeroms, & Delcour, 2003) form double helices much more readily than short or long amylopectin. As the double helices associate in ordered arrays, A, B-, or C-type crystalline structures are packed within the starch. In general, cereal starches have more short amylopectin (DP < 20), which contributes to the formation of A-type crystalline polymorphs. Tuber starches usually have longer amylopectin (DP > 22) and are thereby B-type polymorphs (Bertoft, 2017; Zhu, 2018). C-type crystalline structures (the combination of A- and B-type polymorphs) can be seen in legumes, roots, and some fruit and stem starches. The A- and B-type polymorphic structures are schematically represented in **Figure 1**. The A-type polymorphic (crystalline) structure is packed with fewer water molecules (8

crystalline water), while the B-type polymorph has a more open structure, hydrated with 36-crystalline water molecules. In addition, A- and B-type starches also exhibit a great difference in the distribution of amylopectin branch points (Jane, Wong, & McPherson, 1997). For example, A-type starch clusters its branch points within both amorphous and crystalline regions while B-type starch clusters almost all branch points in the amorphous region. Accordingly, A-type structures have “weak points” derived from the branch linkages present within the crystalline region, making enzymatic digestion much easier in comparison with the B-type starches (Jane et al., 1997). Contrary to the double helix-based crystals, the V-type structure refers to the inclusion of starch with hydrophobic guest molecules such as lipids or polyphenols.

As the double helices and crystals are arranged in an orderly manner, starch forms a semi-crystalline structure (7–11 nm) and a growth ring (100–500 nm) with alternating crystalline (5–8 nm) and amorphous lamellae (2–3 nm) within the native starch granules. The crystalline lamellae forms by the ordered amylopectin clusters of double helices, whereas the amorphous lamellae are the region that contains amylopectin branch points and disordered amylopectin chains. The thickness of the semi-crystalline lamellae depends on the starch type and source (Fan et al., 2014; Kuang et al., 2017; Tan et al., 2017; Wang, Zhang, Chen, & Li, 2016; Yang et al., 2016). A-type starch has shorter amylopectin branch chains (Jane et al., 1997), which contributes to a thinner crystalline lamellae compared with B-type starches (Chi et al.,

2017). Additionally, A-type starch shows a higher susceptibility to acid and enzymatic treatment because the starch contains “weak points” within the crystalline lamellae (Jane et al., 1997). The blocklet, which was observed by Gallant, Bouchet, & Baldwin (1997) and Tang, Mitsunaga, & Kawamura (2006) as clearly defined structures, is also composed of semi-crystalline structures with alternating crystalline and amorphous lamellae (**Figure 1)**. Due to the difficulty of blocklet separation, the fine structures of starch molecules in blocklets are not well described.

Starch granules generally have a size that varies from less than 1 μm (quinoa and dasheen starch) to more than 100 μm (potato starch), which depends on the botanical source of the starch. Starch granules may be round, spherical, polygonal, and irregular depending on the source. However, the shape is always consistent with the morphology of the plant seed or root (*e.g.*, potato starch is ellipsoid-shaped as the potato root shows). Some A-type starches such as waxy corn, common maize, and sorghum are characterized by pores or channels (diameter of 0.07–0.10 mm) penetrating from the external surface towards the hilum (Kim & Huber, 2008). B-type starches are smooth without pore/channels on the granule surface (Kim et al., 2008). Nevertheless, B-type starches such as potato starch also have some porous structures, as estimated using a Surface Area & Pore Size Analyzer (Xie, Li, Chen, & Zhang, 2019). Starch surficial structures from different botanical sources should be further investigated in the future.

3. Updated understanding of starch structures

Starch multi-scale structures have been systematically identified using modern technologies (Huo et al., 2018; Li et al., 2020; Li et al., 2019; Yu et al., 2019; Zhang et al., 2018). In recent years, starch molecular fine structures (amylose and amylopectin fine structures) and starch aggregate structures (amorphous lamellae, crystalline lamellae, fractal structures, and ordered aggregates) have been further investigated (Chi et al., 2018a; He et al., 2020a; Qiao et al., 2019; Qiao et al., 2016; Zhang et al., 2019). The molecular fine structure comprises the chain length distributions (CLDs) of starch branches and whole molecular size distributions (Tao, Li, Yu, Gilbert, & Li, 2019). CLDs are usually measured by size exclusion chromatography (SEC) or coupled with multi angle laser scattering (MALS), fluorophore-assisted capillary electrophoresis (FACE), high performance anion-exchange chromatography (HPAEC), and asymmetrical flow field-flow fractionation coupled with MALS (AF4-MALS). The molecular fine structure is parameterized with a biosynthesis-based model to reveal the changes of starch chain development during starch biosynthesis (Nada, Zou, Li, & Gilbert, 2017). In addition, starch aggregate structures (crystalline structures and lamellar structures) with a size of 1–100 nm can be revealed by X-ray diffraction (XRD), scanning electron microscope (SEM), atomic force microscope (AFM), confocal laser scanning microscope (CLSM), transmission electron microscope (TEM), and mostly by small

angle neutron scattering (SANS) and small angle X-ray scattering (SAXS) (Blazek & Gilbert, 2011). XRD characterizes crystalline structures with a limited-size scale, while AFM, SEM, and TEM focus on the size and morphology of starch nanoparticles. SAXS and SANS are used for characterizing starch structures with a size of several to hundreds of nanometers (Blazek et al., 2011; Zhang et al., 2019). In this review, the progress in understanding starch molecular fine structures and starch nanoscale aggregate structures is updated for further understanding of the changes in starch hierarchical structures during food manufacturing.

3.1. Starch molecular structures

Starch molecular fine structures, including amylose and amylopectin fine structures, are starch basic structures that determine hierarchical structures and functionalities (Tao et al., 2019). CLDs of starch branches obtained by isoamylase pretreatment are usually measured by different techniques including SEC, SEC-MALS, AF4-MALS, FACE, and HPAEC (Castro, Dumas, & Chiou, 2005). SEC separates starch chains by molecular size, specifically, hydrodynamic radius R_h, and provides the molecular weight distribution of molecules, w(log$X$) (Striegel, Yau, Kirkland, & Bly, 2009). R_h can be converted to the corresponding degree of polymerization X using the Mark–Houwink equation, giving $X(R_h)$ (Vilaplana & Gilbert, 2010). SEC accurately determines the molecular weight distribution of amylose or debranched starch chains but cannot give the accurate molecular weight

distribution of amylopectin due to column adsorption and shear degradation. With no stationary phase or packing materials, a wide separation range for size (1nm–50μm), and good compatibility with a variety of solvents, AF4-MALS provides more information about the radius of gyration (R_g), R_h, molecular weight (M_w), apparent density, and conformation (R_g/R_h) of starch molecules (Guo, Li, An, Shen, & Dou, 2019). FACE and HPAEC provide more accurate results and measure the number distribution of molecules *Nde*(X) directly, while both are confined to a relative low degree of polymerization at < ~180 and <~70, respectively (Li, Hu, Tao, Gong, & Yu, 2020). For a linear polymer such as debranched starch, the weight distribution of molecules (w(log*Rh*)) and the corresponding number and distribution of molecules (*e.g.*, *Nde*(X)) are related by $Nde(X)=w(\log X)/X_2$ (Castro, Ward, & Gilbert, 2005). The development of biosynthesis-based models were applied to fit the CLDs data of amylose and amylopectin (Yu et al., 2019). The amylopectin fitting model assumes that the CLDs of amylopectin chains are only determined by the activities of sets of the three starch biosynthesis enzymes: starch synthase (SS), starch branching enzyme (SBE), and starch debranching enzyme (DBE). It also assumes that the amylopectin CLDs are divided into various chain regions *i* (I = 1–3, short, medium, and long region), which are formed by a set of starch biosynthetic enzymes as mentioned above. The final fitting parameters with their biological and structural values are $\beta_{Ap,\,I}$ and $h_{Ap,i}$, i = 1–3. Biological values of the model parameters are the ratio of the enzyme

activities of SBE to that of SS in the enzyme set of *i* (denoted as $\beta_{Ap,i}$) and the relative contribution of that enzyme set to the overall CLDs (denoted as $h_{Ap,i}$). In addition, the model for amylose CLDs with fitting parameters $\beta_{Am,\,I}$ and $h_{Am,\,I}$ (Nada et al., 2017; Yu et al., 2019; Yu, Tao, & Gilbert, 2018) are equivalent to the corresponding quantities $\beta_{Ap,\,I}$ and $h_{Ap,\,I}$ in the amylopectin model. For structural comparison values, a higher β value in a specific fitting region for amylopectin and amylose molecules equals shorter chains, while a higher *h* value denotes a higher amount of chains in this region (Li et al., 2020). Overall, the extended methods and developed models correlated to the starch molecular chains are extremely important to the accurate characterization of the molecular structure of starch, and to obtain starch-based products that exhibit specific functions.

3.2. Starch aggregate structures

3.2.1. Lamellar structures

The SAXS curve of starch correlates with its semi-crystalline structures (crystalline amylopectin lamellae, amorphous amylopectin lamellae, and amorphous amylose background materials) (Cameron & Donald, 1993a,b). Native starch always shows a characteristic peak for the semi-crystalline structures over the SAXS pattern. The SAXS intensity is significantly influenced by the $\Delta\rho$ (the difference in electron density between crystalline lamellae (ρ_c) and amorphous lamellae (ρ_a), $\Delta\rho = \rho_c - \rho_a$) and $\Delta\rho_u$ (the difference in election density between background materials (ρ_u) and

amorphous lamellae (ρ_a), $\Delta\rho_u = \rho_u - \rho_a$) (Cameron et al., 1993a). The increase in $\Delta\rho_u$ concurrently contributes to an elevation of the low-angle intensity and a reduction in the definition of lamellar peak without any changes of the peak position over the SAXS curve, while the increase of $\Delta\rho$ always corresponds to an enhancement in overall intensity, including peak intensity (Tan et al., 2015; Zhang, Li, Liu, Xie, & Chen, 2013b). Based on the changes in SAXS curve, the variation in $\Delta\rho$ and $\Delta\rho_u$ can be extrapolated and in turn, the transformation of starch crystalline lamellae, amorphous lamellae, and amorphous background materials after processing can be revealed (Chi et al., 2017; Zhang et al., 2013b; Zhang et al., 2014a; Zhang et al., 2014b). Accordingly, the changes in starch lamellar structures can be unraveled based on the changes in starch SAXS curves. Zhang et al. (2014b) investigated the changes in starch supramolecular structures during heating in abundant water using the SAXS method. The authors observed an increase of SAXS intensity over the overall curves but a reduction in the definition of the lamellar peak, corresponding to the increase in both $\Delta\rho$ and $\Delta\rho_u$. Generally, starch amorphous background materials absorb water faster than the semi-crystalline lamellae, where the amorphous lamellae are readily hydrated during heating due to the differences in compactness between amorphous lamellae and crystalline lamellae. Accordingly, the changes in SAXS curves revealed the transformation of starch semi-crystalline lamellae, i.e., the greatest destruction of amorphous background, the intermediate destruction of amorphous lamellae, and the

241 weakest destruction of crystalline lamellae during heating in abundant water (Zhang
242 et al., 2014b). By evaluating the changes of SAXS curve, the changes in crystalline
243 amylopectin lamellae, amorphous amylopectin lamellae, and amorphous amylose
244 background materials could be extrapolated.

245 As the alternating amorphous lamellae and crystalline lamellae are rigidly
246 packed within the semi-crystalline regions, starch shows a characteristic lamellar peak
247 over the SAXS curve at *ca*. 0.65 nm^{-1}. The scattering peak area indicates the
248 organization of semi-crystalline lamellae (Qiao et al., 2019; Yang et al., 2019). A
249 larger peak area suggests starch has a higher lamellar ordering (Qiao et al., 2019;
250 Wang et al., 2018; Yang et al., 2019). Integration software are currently used to
251 evaluate the peak area and lamellar ordering, where empirical equations including the
252 Power Law plus Gaussian function (Qiao et al., 2016), the Power Law function plus
253 Lorentzian function (Yang et al., 2019), and the Constant Peak function (Li et al.,
254 2019) can be used for fitting the SAXS curves and calculating the peak area. For
255 further determination of the thickness of semi-crystalline lamellae, crystalline
256 lamellae, and amorphous lamellae, the linear correlation function profile, expressed as
257 the following equation, has been used (Chi et al., 2017; Fan et al., 2014; Wang et al.,
258 2018; Zhang, Chen, Li, Li, & Zhang, 2015).

259 $$f(r) = \frac{\int_0^\infty I(q)q^2 \cos(qr)dq}{\int_0^\infty I(q)q^2 dq},$$

260 where r (nm) is the distance in the real space and q is the scattering vector. The

261 thickness of semi-crystalline lamellae equals the abscissa of the second maximum
262 peak of *f*(r), while the thickness of amorphous lamellae is the abscissa of the solution
263 of the flat *f*(r) minimum and the linear regression curve of the linear region (usually
264 located in the region of $0 < q < 2.5$ nm^{-1}). The thickness of crystalline lamellae is
265 calculated by the difference between the thickness of semi-crystalline lamellae and
266 amorphous lamellae (Fan et al., 2014; Zhang et al., 2015). By revealing the thickness
267 of semi-crystalline lamellae, crystalline lamellae, and amorphous lamellae, the links
268 between starch lamellar features and functionality (such as digestibility and pasting
269 properties) can be well understood (Qiao et al., 2019; Qiao et al., 2019; Qiao et al.,
270 2016; Qiao et al., 2016; Zhang, Li, Chen, & Situ, 2016). This suggests the importance
271 of accurately evaluating starch lamellar features. However, the amorphous
272 background material serves as a third-phase structure within starches, and in turn
273 reduces the accuracy of the linear correlation function to calculate the lamellar
274 parameters of the semi-crystalline lamellae (Zhang et al., 2017). Zhang et al. (2017)
275 fitted the SAXS curve using two Gaussian plus Lorentz functions and resolved the
276 semi-crystalline lamellae-based scattering from the total SAXS pattern of starch. Then,
277 the linear correlation function profile derived from the net lamellar peak profile was
278 obtained to accurately calculate starch lamellar parameters. This improved approach
279 significantly increased the accuracy of determining the thickness of starch
280 semi-crystalline lamellae. Lin, Chi, & Wu (2019) noted that all current studies

281 improperly selected SAXS data to portray the linear correlation function profile
282 because the calculated thickness of amorphous lamellae was smaller than the smallest
283 detectable size extrapolated from the selected data. The necessary SAXS data in the
284 range of $0.1 < q < 2.75$ nm^{-1} were suggested for use in graphing the linear correlation
285 function profiles and avoiding the above mistake. However, increasing the amount of
286 selected data for the analysis also reduced the accuracy of the lamellar parameters due
287 to interference of the amorphous background materials (Lin et al., 2019). It is likely
288 that starch lamellar parameters can be accurately elevated using the combination
289 method of Zhang et al. (2017) and Lin et al. (2019).

290 **3.2.2. Fractal structure**

291 The fractal structure describes the self-similar geometry within starch aggregated
292 scattering objects (Pikus, 2005; Suzuki, Chiba, & Yano, 1997). It is defined as the
293 slope of linear region of the double-logarithmic SAXS curves (Hurd & Flower, 1988;
294 Suzuki et al., 1997). Starch fractal structures are always evaluated by the fractal
295 dimension, which is calculated by the scattering power-law equation: $I \sim q^{-\alpha}$, where
296 the I is SAXS intensity and the α is the exponent used for estimating the fractal
297 dimension. The scattering object is characterized by a surface fractal structure with a
298 fractal dimension $D_s = 6 - \alpha$ if $3 < \alpha < 4$, whereas a mass fractal structure is described
299 with a fractal dimension $D_m = \alpha$ if $1 < \alpha < 3$ (Beaucage, 1995; Hurd et al., 1988;
300 Suzuki et al., 1997). A higher δ indicates the scattering objects have more compact

structures (Suzuki et al., 1997). By evaluating the dimension of fractal structures within scattering objects, starch compactness and ordered structures can be determined (Chi et al., 2017; Zhang et al., 2013b; Zhang et al., 2014a; Zhang et al., 2014b).

3.2.3. Nanoscale reassembled aggregate structures

Native starch granules treated with hydrothermal processes under different moisture contents lose their semi-crystalline structures, with disappeared peaks at *ca*. 0.65 nm^{-1} (Zu et al., 2016; Zhang et al., 2014b). Nevertheless, processed starch shows a shoulder-like peak at *ca*. 0.50 nm^{-1}, corresponding to the reassembly of amorphous starch molecules during cooling due to starch molecule reassembly (Chi, Li, Zhang, Chen, & Li, 2018b; Chi et al., 2020; Li et al., 2019; Sun et al., 2019; Zhang, Li, Janaswamy, Chen, & Chi, 2020). After Lorentz correction (Zhang et al., 2013b), the Kratky plot ($q^2*I(q)$ vs. q) can be obtained to highlight the shoulder-like peak (Chi et al., 2018b; Sun et al., 2019). A peak at finite q over the Kratky plot indicates the presence of ordered structures, and a higher peak area of the Kratky plot suggests more starch nanoscale aggregates (Chi et al., 2018b; Sun et al., 2019). In addition, the size of the ordered nanoscale aggregates can be calculated using the Woolf–Bragg equation ($d=2\pi/q$) according to the Kratky plot peak (Situ, Chen, Wang, & Li, 2014). Zhang et al. (2020) determined that changes in the size of nanoscale aggregates could potentially indicate starch reassembly behaviors, which suggests that nanoscale

aggregates could be used to evaluate starch retrogradation during storage.

4. Effect of starch multi-scale structures on digestibility

Starch digestion has been described in three phases: enzyme diffusion towards the starch, enzyme adsorption onto the starch (formation of the enzyme-starch complex), and the hydrolytic event (Lehmann & Robin, 2007). The underlying mechanism involved in limiting starch digestibility has been classified into two modes: (i) barriers that slow down or prevent access/binding of enzymes to starch, and (ii) starch structures that slow down or prevent enzyme action (Dhital, Warren, Butterworth, Ellis, & Gidley, 2015). Studies have indicated that starch digestion is controlled by different structures. In this review, the effects of starch multi-scale structures on digestibility are comprehensively discussed to guide hierarchical structuration for modulating starch digestibility.

4.1. Amylose and starch digestibility

Amylose and amylopectin serve as the basic components of starch. Its fine structures and the ratio of amylose to amylopectin influence starch chain association and the features of hierarchical structures. Several studies have suggested that amylose is negatively correlated with RDS content but positively correlated with RS content (Cai et al., 2015; Rashmi & Urooj, 2003; Zhang et al., 2007). Lin et al. (2018) investigated the enzymatic hydrolysis of rice starches with the same genetic background. Starches from the same genetic background exhibited the same

amylopectin structures but different amylose contents, varying from approximately 1% to 15%. The results indicated that the starch hydrolysis rate slowed, and the extent was reduced when amylose content increased. Further research showed that the amylose chain-length distribution data could be fitted by a mathematical model (Nada et al., 2017). The data were then parameterized in terms of a small number of biologically meaningful parameters to analyze the correlation between amylose fine structure and *in vitro* starch digestibility (Nada et al., 2017). Yu et al. (2018) suggested that the content of shorter amylose chains and total amylose molecular size were negatively correlated to starch digestion rate via modelling of amylose chain length distribution. Gong, Cheng, Gilbert, & Li (2019) revealed that rice starch digestibility could be slowed via the modification of amylose fine molecular structure (i.e., increasing the amount of amylose short-medium chains) rather than just altering the amylose content. The interactions of amylose short-medium chains contributed to form the smaller gel network cells in the retrograded starch, which significantly slowed starch digestion (Gong et al., 2019).

During food processing (cooking, steaming, baking, and frying), amylose may influence starch structural transformation and enzyme digestion. **Figure 2** shows the possible structural changes of high amylose-containing starches during cooking and enzymatic digestion. High amylose-containing starches are more thermostable than the low amylose-containing sample because amylose retards starch swelling and

disruption during processing (**Figure 2**) (Liu, Yu, Xie, & Chen, 2006). This in turn allows a high possibility for high amylose-containing starches to retain a semi-crystalline structure during conventional cooking, which suppresses enzyme access/binding with starch to reduce digestibility (Martinez et al., 2018; Tester et al., 2006). In addition, amylose that leaches from starch granules tends to form reassembled ordered structures during cooling and digestion. Starch with higher amylose rearranges into a higher ordered structure in comparison with low amylose-containing starch during cooling (Fredriksson, Silverio, Andersson, Eliasson, & Åman, 1998) because amylose reassociates gel networks containing stable double helices and strong crystallites (Alhambra et al., 2019). Witt, Gidley, & Gilbert (2010) additionally suggested that amylose retrogradation may occur and form reassembled ordered structures during the digestion process. Reassembled, ordered amylose structures thereby reduce enzyme accessibility to the starch surface and enzymatic catalyzation (Dhital et al., 2015). If hydrophobic guest molecules such as lipids are available in the system, the leached amylose also binds with lipids to form amylose-lipid inclusion complexes, which do not fit into the active sites of α-amylases. Therefore, the amylose-lipid complexes belong to the enzyme-resistant fractions (Alhambra et al., 2019; Sun et al., 2019). The formation of reassembled structures involving amylose–amylose and amylose–lipids during cooking, cooling, and digestion could be a key action of amylose that affects starch digestibility. However,

Hung et al. (2016) showed that amylose content did not affect the *in vivo* digestion of starch following heat-moisture treatment, suggesting that the interactions of amylose–amylose, amylopectin–amylopectin, and amylose–amylopectin chains were responsible for starch chain accessibility to hydrolyzing enzymes. The aggregate assemblies of starch, rather than the structures or content of amylose, may determine starch *in vivo* digestion (Hung et al., 2016). How amylose affects *in vivo* starch digestion should be further investigated.

4.2. Amylopectin and starch digestibility

Many studies indicate that amylopectin chain length in starch correlates with starch digestion (Miao et al., 2014b; Wang, Zhang, Chen, & Zhong, 2020). Starch treated with maltogenic α-amylase showed an increased content of amylopectin with DP < 13 and α-1,6 linkages, which significantly increased starch resistance to enzymatic hydrolysis due to the bulky steric hindrance (Miao et al., 2014b; Miao et al., 2014c). Pretreatment with a branching enzyme yielded an increase in the content of α-1,6 linkages and a reduction in RDS content (Li et al., 2018). Moreover, amylopectin has been reported to have a critical effect on starch crystalline structures such as polymorph type and crystallinity (Li & Zhu, 2017; Zhu, 2018). Amylopectin with DP 13–24 and 25–36 promoted the formation of rigid and crystalline structures, which significantly suppressed enzymatic digestion (Kim et al., 2013; Zhu, 2018). Pretreatment with amylosucrase or pullulanase–amylosucrase created such

amylopectin and increased the perfection and rigidity of crystalline structures, thus slowing starch digestion (Zhang, Wang, Chen, & Zhong, 2019).

During food processing, amylopectin structures affect starch structural transformation as well as starch digestibility. Intact or densely-packed structures (double helices and crystals) packed by the amylopectin show stronger resistance to enzymatic hydrolysis in comparison with those that are amorphous (Miao, Zhang, Mu, & Jiang, 2010). During cooking, ordered hierarchical starch structures are progressively disrupted (Wang & Copeland, 2013) and the molecular structures and their assembly critically influence cooked starch digestibility (Syahariza, Sar, Hasjim, Tizzotti, & Gilbert, 2013). Srichuwong, Sunarti, Mishima, Isono, & Hisamatsu (2005) also analyzed the contribution of amylopectin fine structures to enzymatic digestibility of starches from different botanical sources. They demonstrated that the enzymatic hydrolysis of both gelatinized and retrograded starches positively and negatively correlated with the DP 8–12 and DP 13–26 amylopectin chains, respectively. Overall, amylopectin with long chain length, especially the fractions with DP > 13, contributed to low starch digestibility. Benmoussa, Moldenhauer, & Hamaker (2007) and Shen, Bertoft, Zhang, & Hamaker (2013) suggested that long amylopectin tended to form double helices or crystallites during cooling and retrogradation, contributing to low digestion as shown in **Figure 2**. Elongating amylopectin chain length, mostly by amylosucrase, has been attracting great interest

421 in reducing starch digestibility (Kim, Kim, Moon, & Choi, 2014; Kim et al., 2013;
422 Kim, Choi, Park, & Moon, 2017; Kim, Kim, Choi, Park, & Moon, 2016). However, a
423 suitable chain length of amylopectin is required for packing ordered and crystalline
424 structures. Amylopectin branch chains with DP *ca*. 12–24 easily form double helices
425 and crystalline structures in native and retrograded starches, while the fractions with
426 DP 6–9 inhibit the assembly of ordered structures (Zhu, 2018). Alhambra et al. (2019)
427 validated the strong positive (r = 0.95) and negative (r = -0.83) correlation between
428 DP 6–12 and DP 13–24 amylopectin chains, respectively, with the hydrolysis rate of
429 retrograded rice starch, which determines the *in vitro* digestion rate of starch.
430 Available studies also indicate that starch digestibility is negatively correlated with
431 amylopectin with DP *ca*. 12–24. Lin et al. (2016) investigated the relationship
432 between the molecular structures and enzyme hydrolysis properties of maize starch
433 varying in amylose content. Pearson correlation analysis revealed that the RDS
434 content of native, gelatinized, and retrograded starches positively correlated with the
435 amylopectin branch-chains with DP 6–12 and 13–24, where it was negatively
436 correlated with amylopectin branch-chains with DP 25–36 and ≥ 37. It should be
437 noted that the starches used by Lin et al. (2016) significantly differed in amylose
438 content. As we discussed in the section on amylose and starch digestibility, amylose
439 also significantly correlates with starch digestibility. The differences in the
440 digestibility of starches may be critically determined by amylose content, and the

Pearson coefficients may indicate the same changes in structure and digestibility. Liu et al. (2018) obtained different fine structure-containing cassava starches by controlling the cassava growth period and revealed the role of molecular fine structures on the digestibility of cooked starch. The authors suggested that RS content positively correlated with amylopectin branch-chains with DP 25–36. Furthermore, they also noted that the amylose content strongly correlated with RS content. Due to the difference in amylose content and amylopectin fine structures in the study, it was difficult to reveal how the key structures determine starch digestibility. Kim, Choi, Choi, Park, & Moon (2020) characterized the chain length of RDS+SDS+RS, RDS-removed starch, and RS, to investigate how amylopectin fine structures influence starch digestibility. Results showed that decreases in short chains (DP 6–12) and long chains (DP 25–36) were observed with the removal of the SDS fraction, while the very long chains (DP ≥ 37) were unchanged and the middle chains (DP 13–24) significantly increased. Accordingly, the authors suggested that RDS included the singular amylose chains or amorphous double helices that were not long enough or not aligned in an ordered structure, SDS were likely the short chains (DP 6–12) and ordered structures that were packed by double helices with DP 25–36, and RS was the semi-crystalline or crystalline fractions assembled by double helices with DP 13–25, DP ≥ 37, and some helices with DP 25–36 (Kim et al., 2020).

In addition, the shortening of amylopectin by *β*-amylase also contributes greatly

461 to the reduction of starch digestibility (Miao et al., 2014). Miao et al. (2014) partially
462 hydrolyzed starch using *β*-amylase and analyzed how this influenced starch
463 digestibility. By continuously prolonging the time of enzymatic catalyzation,
464 amylopectin fractions with DP < 13 significantly increased, initially yielding
465 decreased starch digestibility and increased SDS content but then increasing
466 digestibility and decreasing SDS content. Zhang, Ao, & Hamaker (2008) also
467 observed a parabolic relationship between starch molecular structure and starch
468 digestibility, suggesting that starch with a high fraction of DP < 13 or a high
469 proportion of long amylopectin of DP ≥ 13 has a high SDS content. Although short
470 amylopectin has a low possibility of forming double helices, branch distances at the
471 lower end of the distribution allows for a strong ability to retard enzyme catalysis due
472 to the steric hindrance (Li et al., 2017). Moreover, a suitable length starch chain is
473 needed for the binding of starch with the enzyme active sites (Carolie, Jean-Pierre,
474 Guy, Christian, & Françoise, 1996; Robyt, 2009).

475 **4.3. Short-range ordered structure and starch digestibility**

476 The FTIR absorption bands at 1047 and 1022 cm^{-1} are ascribed to the presence of
477 C-O-H bending and -CH_2-related modes. As those two bands are sensitive to the
478 amount of ordered or crystalline structures and amorphous structures of starch,
479 respectively, the absorbance ratio of 1047/1022 cm^{-1} is used to evaluate the
480 short-range ordered structures in starch (Chi et al., 2017; Soest, Tournois, de Wit, &

481 Vliegenthart, 1995; Wang, Sun, Wang, Wang, & Copeland, 2016). The Raman peak at
482 480 cm^{-1} is also used to determine starch short-range ordered structure by calculating
483 the area or full width at half maximum of the band, in that the peak relates to the
484 -CH_2- mode (Wang et al., 2018; Wang et al., 2016). A higher $R_{1047/1022}$ or a lower
485 FWHM (FWHM, full width at half maximum) indicates the starch sample contains
486 more short-range ordered structures.

487 The short-range ordered structures of processed starches are the key factor in
488 starch structuration and enzyme digestion. Our research indicated that starch gel
489 containing more short-range ordered structures showed a stronger ability to suppress
490 enzyme diffusion toward the starch surface and to reduce cooked starch digestibility
491 (Chi et al., 2019b). In addition, our research also investigated the correlation between
492 the short-range ordered structures of starch pastes and digestibility, and found that
493 SDS and RS content was highly associated with short-range ordered structures (Chi et
494 al., 2019a). Starch rich in RS content had more short-range ordered structures
495 compared with those with high SDS (Chi et al., 2019a). In addition, complexing with
496 non-starchy compounds increased short-range ordered structures such as
497 hydrocolloids, protein, and phenolic compounds during cooking. Pullulan and pectin
498 adhered around the starch granules, retarding the disruption of short-range ordered
499 structures and crystalline structures and slowing starch digestion (Chen et al., 2019).
500 Guar gum promoted the reassembly and molecular interactions of tapioca starch and

501 decreased starch digestion rates (Hong et al., 2016). Further research demonstrated
502 that guar gum promoted the formation of short-range ordered structures and
503 crystalline structures via interaction with starch molecules, and in turn mitigated
504 starch digestion by reducing RDS fractions (Zheng et al., 2019). Proteins also have
505 the ability to increase short-range ordered structures and reduce starch digestion.
506 Potato protein isolate inhibited starch granule swelling and disruption, resulting in
507 more short-range ordered structures and low digestibility after cooking (Lu, Donner,
508 Yada, & Liu, 2016). Whey protein potentially interacted with corn starch during
509 cooling, which resulted in an increase in short-range ordered structures and a
510 significant reduction in RDS content (Yang, Zhong, Goff, & Li, 2019). Green tea
511 polyphenols enabled the formation of V-type inclusion complexes, contributing to an
512 increase in short-range ordered structures and a decrease in starch digestion rates
513 (Zhao et al., 2019a; Zhao, Wang, Zheng, Chen, & Guo, 2019b).

514 Previous studies indicated that short-range ordered structures usually have a high
515 resistance to enzyme catalyzation owing to their suppression of the access/binding of
516 enzymes to starch molecules (Dhital et al., 2015; Lin et al., 2015). However,
517 short-ranger ordered structures do not always determine starch digestibility. Wang et
518 al. (2018) determined the short-range ordered structures and digestibility of
519 cooked-starches treated with heat-moisture, with varying moisture contents. As the
520 moisture content increased, the heat-moisture treated starches exhibited a continuous

reduction in short-range ordered structures but a significant decrease in starch digestibility with RDS reduction and RS elevation. Heat-moisture treatment contributed to partial gelatinization of the starch surface and then an increase in starch digestibility. Nevertheless, it also caused the formation of reassembled ordered molecular aggregation architecture, which increased crystalline perfection and improved resistance to hydrothermal or enzymatic treatment (Wang et al., 2018). Compared with long-range ordered structures, short-range ordered structures exhibited a weaker effect on starch digestibility (Pu et al., 2013; Sun et al., 2019; Wang et al., 2017). Long-range ordered structures significantly correlated with the access/binding behaviors of enzymes to starch (Wang et al., 2017). Wang et al. (2017) showed that short-range ordered structures of cooked starch following hydrothermal treatment did not determine the access/binding of enzymes to starch. However, long-range ordered structures correlated with substrate accessibility and the occurrence of enzymatic catalytic hydrolysis (Wang et al., 2017). Sun et al. (2019) and Pu et al. (2013) also indicated that short-range ordered structures were irrelevant to starch digestibility because long-range ordered structures such as crystalline structures and ordered reassembled structures limited enzyme access to the starch surface. Overall, short-range ordered structures might determine the digestibility of amorphous or low ordered structure-containing starches but might not significantly correlate with the digestibility of starch which contains relatively ordered long-range

structures.

4.4. Helical structures and starch digestibility

Amylose and amylopectin arrange and form densely-packed single and double helices, respectively. As these two types of starch structures are being arranged, a highly ordered crystalline matrix can be formed. Densely-packed structures always show a strong resistance to enzymatic hydrolysis, whereas the amorphous region tends to be easily hydrolyzed (Tian et al., 2018). According to the hydrolysis mode of porcine pancreatic α-amylase delineated by Carolie et al. (1996), the enzyme has five subsites that bind starch, and each subsite requires binding to at least three glucose-units before cleaving an α-(1,4)-glycosidic bond. When starch chains are densely packed into single or double helical structures, the densely-packed matrix protects glycosidic linkages from the attack of amylolytic enzymes, thereby decreasing the available number of binding sites (Carolie et al., 1996). According to a previous study (Chen et al., 2017), starch digestibility was reduced as a function of helical content because the dense structures enabled glycosidic bonds to avoid enzymatic hydrolysis. In addition, perfectly-packed helical structures showed high resistance to enzymatic attack and in turn, increased RS content. Alternatively, helical structures with imperfect association were slowly digested to mainly yield an increase in SDS content (Zhang et al., 2008). Non-starchy ingredients such as lipids and polyphenols potentially promote the formation of single or double helical structures

561 via non-covalent interaction (*e.g.*, hydrophobic interaction) with starch molecules,
562 contributing to a significant reduction in digestion rate (Guo et al., 2019).

563 The thermal stability of the helical structure plays an important role in processed
564 starch digestibility. Starch enthalpy has been negatively correlated with the ratio of
565 short B-chains to long B-chains (Li et al., 2017). Fractions with more short chains (DP
566 < 6) contribute to low thermal stability of the helical structures (Vamadevan, Bertoft,
567 & Seetharaman, 2013; Vamadevan, Bertoft, Soldatov, & Seetharaman, 2013). The
568 long branch-chains in starch granules result in an increase in the stability of helical
569 structures, causing a higher gelatinization temperature (Chung, Liu, Lee, & Wei,
570 2011). This allows the thermostable-starch a higher ability to retain its ordered
571 structures after conventional cooking (Chung et al., 2011), in turn protecting the
572 binding sites of the starch molecules from enzymatic hydrolysis.

573 **4.5. Crystalline structures and starch digestibility**

574 As the helical structures are oriented in a specific mode, starch is densely packed
575 with A-, B-, C-, and V-type polymorphs. Compared with amorphous regions, the
576 crystalline structures show a high resistance to enzymatic hydrolysis because the
577 supramolecular structures of the crystalline matrix are protected from enzyme
578 hydrolysis. The starch chains must properly fit into the enzyme active sites after the
579 enzyme is absorbed onto starch to allow catalyzation of glucosidic bonds. When
580 crystalline structures do not melt below the gelatinization onset temperature, the

crystallinity and crystalline type of the polymorphs play an important role in starch digestibility (Zeng et al., 2014). By increasing the crystallinity of starch samples, the digestibility is reduced (Miao et al., 2009; Zeng et al., 2014). Owing to the "weak points" within crystalline structures, A-type starch tends to have a high enzyme susceptibility (Jane et al., 1997) where the B-type starch has a lower digestion rate and extent compared to the A-type starch due to the well-defined polymorph structures. The C-type polymorph, which is a combination of A- and B-type polymorphs, has an intermediate enzymatic susceptibility between A- and B-type polymorphs. Regarding the V-type structured starch fractions, the bulk molecular structures protect starch binding sites from enzyme active pockets. This is due to the stable complexes formed when amylose or long amylopectin bind with hydrophobic guest molecules through hydrophobic interaction (Raigond, Ezekiel, & Raigond, 2015). Thereby, V-type starch fractions serve as typical resistant starches (Dupuis et al., 2014).

Starch crystalline structures are significantly disrupted along with a reduction in crystallinity during food processing, which yields an increase in starch digestion rates. When starch is heated above the gelatinization onset temperature, the crystalline matrix begins melting and in-turn increases the number of starch binding sites for enzymes. Gelatinized starch, which contains more loose starch structures, is much more susceptible to enzyme attack than the corresponding native starch (Wang et al.,

601 2018). Gelatinized starch decreases the crystallinity and ordered structures, thereby
602 increasing enzyme diffusion onto the starch substrate (Dhital et al., 2015). The loose
603 structures provide more binding sites for enzymes to increase starch digestibility (Tian
604 et al., 2018). A thermostable starch (starch defined with a perfect crystalline structure),
605 has a high gelatinization onset temperature, which results in a high possibility of the
606 starch retaining its semi-crystalline structure after cooking (Li, Gidley, & Dhital,
607 2019). Accordingly, the thermostable crystalline polymorphs (perfectly-packed
608 crystals) may retain their ordered and dense matrix after cooking and show a high
609 resistance to enzyme diffusion, binding, and catalyzation toward starch molecules,
610 possibly reducing RDS content but increasing RS content. V-type starch structures,
611 (complexes formed by the amylose or long amylopectin with hydrophobic factors) are
612 thermostable during cooking. This restricts starch swelling during cooking (Wang et
613 al., 2020) and retards the breakdown of intact structures, limiting the accessibility of
614 digestive enzymes to starches. Sun et al. (2019) and Chi et al. (2018a) determined that
615 starches coupled with lipids or other hydrophobic guest molecules have a
616 gelatinization onset temperature higher than 79.70 ^{o}C, which enables the inclusion
617 complexes to retain intact structures after cooking. Particularly, the type II inclusion
618 complexes, which have a gelatinization temperature above 100 ^{o}C, are more likely to
619 undergo conventional hydrothermal treatment and keep their ordered structures to
620 reduce enzymatic attack (Chi et al., 2018a; Sun et al., 2019). Cooked starch can

621 reassemble with non-starchy ingredients (i.e. lipids and polyphenols) and form
622 crystalline structures, which slows starch digestion significantly. Rice starch forms
623 V-type complexes with gallic acid and increases starch ordered structures by
624 non-covalent interactions, reducing the accessibility of starch molecules to digestive
625 enzymes (Chi et al., 2019b; Liu, Chen, Xu, Liang, & Zheng, 2019).
626 Proanthocyanidins (PA) interact with starch and form V-type inclusion complexes,
627 contributing to a significant increase in RS content (Amoako & Awika, 2019). Lipids
628 interact with starch chains through hydrophobic interactions that yield the formation
629 of starch–lipid inclusion complexes during cooking. Lotus seed amylose-fatty acid
630 complexes were shown to form during high hydrostatic pressure treatment, which
631 contributed to a reduction in starch enzymatic digestion rate (Guo et al., 2019). The
632 chain length of fatty acids significantly affects their interactions with starch, in turn
633 determining the formation of starch–fatty acids complexes and changes in starch
634 digestibility (Chen et al., 2018).

635 Increased starch crystallinity yields a reduction in starch digestibility but may
636 increase both SDS and RS content based on the features of crystalline structures. The
637 increased V-type crystals were significantly correlated with increased RS content (Chi
638 et al., 2018a; Dupuis et al., 2014). Starch that is perfectly packed significantly retards
639 enzyme accessibility to the starch surface, resulting in high resistance to enzymatic
640 hydrolyzation (Wang et al., 2018). However, starch with imperfect association and

641 crystallization structures has been shown to be slowly digested (Chi et al., 2019a;
642 Zhang, Sofyan, & Hamaker, 2008; Li et al., 2019; Zhang et al., 2008; Zhang, Hu, Xu,
643 Jin, & Tian, 2011). Herein, the perfectly packed crystals might highly associate with
644 RS content, while imperfectly packed crystals significantly link to SDS content.

645 **4.6. Lamellar structures and starch digestibility**

646 Starch semi-crystalline structures are packed by alternating crystalline and
647 amorphous lamellae. The amorphous lamellae can be quickly digested due to the
648 existence of amylopectin branch points and disordered amylopectin/amylose chains
649 (Xie et al., 2020; Zhang et al., 2014b). The crystalline lamellae have a higher bulk
650 density of molecule chains than the amorphous lamellae within the semi-crystalline
651 region (Qiao et al., 2019; Qiao et al., 2019). Accordingly, starch crystalline lamellae
652 was digested less than the amorphous lamellae (Jane et al., 1997). By increasing the
653 thickness of the crystalline lamellae, starch digestibility was reduced because the
654 compact crystalline structure suppressed the diffusion of the enzyme toward the starch
655 substrate (Zhang et al., 2016). Crystalline lamella also conceals starch binding sites
656 within densely packed structures, thus decreasing the binding of enzyme active sites
657 to starch molecules. Subsequently, starch crystalline lamellae resulted in low
658 catalyzation and a significant increase in RS content (Qiao et al., 2019; Qiao et al.,
659 2019; Zhang et al., 2016). Amylopectin with different chain lengths contributes to the
660 difference in features of crystalline lamellae in that crystalline lamellae packed with

661 short amylopectin is thinner and contains more “weak points” (regions sensitive to
662 enzymes) than those with long amylopectin (Wang et al., 2016). Therefore, starch
663 crystalline lamellae exhibits different enzymatic digestion behaviors because of the
664 differences in amylopectin fine structures. Jane et al. (1997) suggested that the
665 crystalline lamellae of A-type starch could be slowly digested because of the “weak
666 points” within crystalline lamellae. A-type starch clusters its branch points in both
667 amorphous and crystalline regions, and the branch linkages presented in the
668 crystalline region significantly promote enzymatic digestion (Jane et al., 1997).
669 Compared with A-type starch, B-type starch had the most branch points scattered in
670 the amorphous lamellae, making it less susceptible to enzymatic hydrolysis. Thus, it
671 seems that the perfectly-packed crystalline lamellae are highly resistant to enzyme
672 attack and increased RS content, while the imperfectly-packed crystalline lamellae are
673 slowly digested and yield an increase in SDS content. Due to the difficulty of the
674 separation of blocklets, there is a dearth of information on the roles of crystalline and
675 amorphous areas in blocklets in digestibility. However, it can be speculated that the
676 crystalline and amorphous structures in the blocklets have a similar effect on
677 digestibility compared with the crystalline and amorphous structures within the
678 growth rings because the structural basis for all crystalline and amorphous areas is
679 identical (Huang et al., 2017; Huang, Wei, Li, Liu, & Yang, 2014; Tang et al., 2006).

680 Starch gelatinization is always associated with the breakdown of starch

semi-crystalline structures during heating, especially the crystalline lamellae (Xu, Blennow, Li, Chen, & Liu, 2019). In this way, starch crystalline lamellae melts and the bulk density decreases, which promotes enzyme binding with starch. Nonetheless, starch with thicker crystalline lamellae may maintain more ordered structures after cooking and thus have lower digestibility (Chi et al., 2017; Liu et al., 2018; Wang et al., 2018; Wang et al., 2016). Starch complexation with oleic acid/linoleic acid during heat-moisture treatment resulted in a significant reduction in the thickness of amorphous lamellae and an increase in ordered molecular chain aggregations in the amorphous amylose background area. This causes the starch to retain its ordered structures during cooking and to increase RS content (He, Zheng, Wang, Li, & Chen, 2020b). Importantly, starch digestibility is closely related to the interplay of many structural factors except lamellar structures. The enzymatic digestion behaviors of cooked starch is sometimes irrelevant to lamellar features but is more dependent on the internal structures in the lamellae such as crystalline structures (Tan et al., 2017) and well-defined helical structures (Liu, Zhang, Chen, Li, & Zheng, 2019).

4.7. Fractal structure and starch digestibility

The compactness of starch internal structures can be extrapolated according to the dimension of fractal structures (Zhang et al., 2013b). Surface fractals have a higher compactness than mass fractals (Chi et al., 2017; Tan et al., 2015; Zhang et al., 2013b). Previous studies have determined that the density of starch structures is

negatively correlated with digestibility because the ordered structures significantly retard enzyme diffusion onto the starch surface and binding with starch molecules (Dhital et al., 2015; Tian et al., 2018). A high value of fractal dimension suggests that starch is densely packed and possibly has lower digestibility (Chen et al., 2018). Li et al. (2019) and Qiao et al. (2016) reported that fractal structure with a high fractal dimension (high compactness) contributes to a reduction in starch digestibility. Our group also suggested that starch with a fractal dimension of 1.73–1.90 has lower digestibility than starch with a lower fractal dimension of 1.13 (Liu et al., 2019). In addition, our previous study investigated the correlation between fractal structure and RDS, SDS, and RS content using Pearson matrix (He et al., 2020a). Results suggested that the fractal dimension negatively correlated with RDS (-0.994, $P < 0.01$) but positively correlated with SDS (0.999, $P < 0.01$) and RS (0.985, $P < 0.05$) (He et al., 2020a). This suggests that the compactness of starch internal structures significantly influences starch digestibility.

4.8. Reassembled aggregate structure and starch digestibility

After food processing, starch molecules form new multi-scale structures which determine the digestibility of the processed starch. Cooked starch reassembles into ordered aggregates in terms of retrogradation and reassociation with non-starchy factors (lipids, protein, and polyphenols) after gelatinization, significantly mitigating digestibility (Tian et al., 2018; Zhang, Chen, Zhao, & Li, 2013a). Reassembled

crystals and helical structures show a lower susceptibility to enzymatic attack and slower digestion (Tian et al., 2018; Zeng et al., 2015). In addition, starch reassembly yields the formation of nanoscale aggregate with a size of *ca*. 15 nm (Li et al., 2019; Situ et al., 2014; Zhang et al., 2020). Our previous work indicated that the content of nanoscale aggregate positively correlated with starch resistance to enzyme digestibility (Chi et al., 2018b; Situ et al., 2014; Sun et al., 2019). Starch with a higher content of reassembled nanoscale aggregate exhibited lower enzymatic digestibility (Chi et al., 2018b; Li et al., 2019; Situ et al., 2014; Sun et al., 2019). According to Zhang et al., (2020), the reassembled aggregate increased in size during retrogradation, indicating the size of reassembled aggregate changes during starch reassociation. However, how the size of reassembled aggregate influenced starch digestibility remains unresolved because limited studies have been conducted on the correlation between reassembled aggregate and starch digestibility. More studies should be conducted to determine the effect of reassembled aggregate on starch digestibility.

5. Principles for targeted regulation of starch digestibility

Numerous studies have demonstrated that starch multi-scale structures are related to digestibility and play an important role in human nutrition. The long-term consumption of RDS-rich foods results in a high risk for the occurrence of metabolic chronic diseases (Ludwig, Hu, Tappy, & Brand-Miller, 2018). Thus, there is a need to establish the principles of targeted regulation of starch digestibility and slowed

741 digestion rate or resistance to digestion. The key structures for slowing starch
742 digestion are summarized in **Figure 3**. Starch enzymatic hydrolysis was suppressed
743 by increasing the content of lipids, proteins, highly branched-amylopectin, long
744 amylopectin helices (DP > 13), amylose fractions, double helices, short-range ordered
745 structures, V-, A- or B-type crystals, and nanoscale reassembled aggregates, the
746 ordered degree and compactness of starch structures and the thickness of
747 semi-crystalline lamellae and crystalline lamellae. However, SDS and RS exhibit
748 different nutritional and physiological attributes in the human diet (Miao et al., 2015a;
749 Zhang et al., 2009; Bindels et al., 2015; Duan et al., 2019; Rehman et al., 2012). Thus,
750 the rational design of starch structures is more important for targeted preparation of
751 SDS- or RS-enriched foods to meet different dietary requirements. Above all, we
752 must clearly identify the key structures significantly involved with SDS and RS.

753 According to the comprehensive discussion about the relationship between starch
754 multi-scale structures and digestibility, it can be concluded that SDS has
755 highly-branched molecular features or relatively ordered fractions, RS is the structure
756 that includes well-defined and perfectly-packed starches, and RDS exhibits
757 amorphous structures. The schematic diagram of the molecular features of RDS, SDS,
758 and RS is shown in **Figure 4** and **Table 1**. To be more specific, SDS is a starch with
759 high α-1,6 linkages (Miao, Li, Huang, Jiang, & Zhang, 2015b; Miao et al., 2014a;
760 Miao et al., 2014), short branch chains (DP < 13) (Zhang et al., 2008), long chains

761 with DP 25–36 (Kim et al., 2020), or imperfect helical and crystalline structures (Liu
762 et al., 2017; Zhang et al., 2013a). Additionally, our group and other researchers have
763 suggested that lamellar structures or reassembled aggregate structures with
764 imperfectly packed regions (A-type “weak points” and imperfect double helices as
765 shown in **Figure 3**) can be slowly digested (Jane et al., 1997; Qiao et al., 2016; Zhang
766 et al., 2016). RS is rich in high amylose content (Li et al., 2019), double
767 helix-promoting chains with DP *ca*. 12–24 (Vandeputte et al., 2003; Vermeylen et al.,
768 2006), and DP ≥ 37, along with some chains with DP 25–36 (Kim et al., 2020),
769 perfectly-packed double helices and crystalline structures (Pu et al., 2013; Sun et al.,
770 2019; Zhang et al., 2013a), V-type crystals (Tan & Kong, 2019), or densely-packed
771 crystalline lamellae and more ordered reassembled aggregate structures (Qiao et al.,
772 2019; Qiao et al., 2016; Qiao et al., 2016; Zhang et al., 2016). In addition to the chain,
773 helical, crystalline, and lamellar structures, our group also suggested that short-range
774 ordered structures and fractal structures significantly correlate with SDS and RS
775 content (Chi et al., 2019a; Chi et al., 2017; Chi et al., 2019b; He et al., 2020a; Sun et
776 al., 2019; Wang et al., 2016). The short-range ordered structure may not always
777 significantly correlate with SDS and RS content because the long-range ordered
778 structures critically determine starch digestibility (Pu et al., 2013; Sun et al., 2019).
779 However, gelatinized starches with relatively low and high content of short-range
780 ordered structures have high SDS and RS content, respectively (Chi et al., 2019a; He

et al., 2020a). Starch that is packed with ordered structures but relatively low compactness contains a high content of SDS (Zhang et al., 2016), while the starch packed with a high compactness by the ordered structure yields a high RS content (He et al., 2020a). According to these principles and the key multi-scale structures of SDS and RS, starch that targets nutritional and physiological attributes can be rationally designed through structuration. This can be done through the design of suitable helical, crystalline, lamellar, fractal, and reassembled aggregate structures at different length scales using specific starch molecules. In this way, the functionalities of starchy foods could ultimately be reasonably modulated.

6. Conclusions and future perspectives

Enriching our understanding of starch structuration principles can guide the mitigation of starch digestibility and targeted preparation of SDS- and RS-fortified foods. The information presented in this review suggests the fundamental importance of considering the effect of starch multi-scale structures on digestibility, especially the SDS and RS formation, and the basic principles of starch structuration and design for modulating digestibility. Amylose and amylopectin fine structures, short-range ordered structures, helical and crystalline structures, lamellar and fractal structures, and the newly-formed aggregated structures during food processing determine enzymatic digestion. Amylose, amylopectin with DP < 13 and DP 13–24, short-range ordered structures, and well-defined helical, crystalline, and lamellar structures are

801 particularly effective at reducing the rate and extent of enzymatic digestion. In
802 particular, faulty- and perfectly packed helical, crystalline, and lamellar structures are
803 proposed to be SDS and RS, respectively. The hierarchical structures of starch are
804 thereby intrinsically linked and driven by starch intermolecular interactions with
805 different characteristics, suggesting that starch digestibility does not always correlate
806 with the sole structure but also the whole multi-scale structure. Therefore, to realize
807 targeted regulation of starch digestibility and targeted preparation of specific
808 digestibility foods, the systematic design of starch multi-scale structures is urgently
809 needed.

810 However, the digestibility and multi-scale structures of starch in foods is
811 complex, and further studies are needed to precisely design starch structures to
812 modulate starch digestibility. Current *in vitro* studies do not generally focus on mouth-
813 and gastric digestion. Nevertheless, mouth-simulated processing may change starch
814 microstructures due to chewing and salivary amylase digestion, and gastric-simulated
815 digestion also hydrolyzes starch owing to acid hydrolysis and salivary amylase
816 hydrolysis (Freitas, Feunteun, Panouille, & Souchon, 2018). Thus, mouth- and
817 gastric-simulated processes are needed for starch *in vitro* digestion analysis. Although
818 amylose has been confirmed to positively correlate with RS content, as was
819 determined by *in vitro* digestion, amylose content does not affect *in vivo* digestion
820 (Hung et al., 2016). The difference between the *in vitro* and *in vivo* digestion of starch

821 has been investigated and it was determined that the RDS and SDS content is likely to
822 be different after each type of digestion (Hasjim, Lavau, Gidley, & Gilbert, 2010).
823 There are limited studies focused on how the starch structures influence *in vivo*
824 digestibility. More studies should be conducted to determine the roles of starch
825 multi-scale structures on *in vivo* digestibility to increase understanding of the
826 nutritional attributes of structured starch. First, the relevance between *in vitro* and *in*
827 *vivo* studies to starch digestibility should be established to increase understanding of
828 the nutritional attributes of structured starch. Second, the starch multi-scale structures
829 in starchy food systems consumed in daily life should be further investigated.
830 Although starch key structure-digestibility relationships have been comprehensively
831 summarized, how starch structures in real food systems influence the digestibility
832 have been rarely studied. Starch structures of ready-to-eat starchy foods ultimately
833 determine starch digestion. Thus, starch structures in real foods on the table and their
834 correlated effects on the starch digestibility should be investigated. Finally, different
835 personalized groups may require different starch digestion behaviors. For example,
836 starch in infants and the elderly should be easily enzymatically digested while in
837 young people starch should be slowly digested or even resistant to digestion, to meet
838 the requirements of human wellness. Addressing the key structures associated with
839 different enzymatic digestion behaviors, future study on the rational design of starchy
840 foods with specific digestibility for personalized groups such as people of different

ages or with special dietary and health care needs is suggested.

Acknowledgments

This work was supported by the National Natural Science Foundation of China (31771930, 32072172).

Author contributions

Chengdeng Chi: investigation, literature analysis, writing and editing; Xiaoxi Li: conceptualization, supervision, reviewing and editing; Shuangxia Huang, Ling Chen, Yiping Zhang, Lin Li and Song Miao: reviewing and editing.

Declaration of competing interest

The authors declare no competing financial interest.

852 **References**

853 Alhambra, C. M., de Guzman, M. K., Dhital, S., Bonto, A. P., Dizon, E. I., Israel, K. A.
854 C., Hurtada, W. A., Butardo, V. M., & Sreenivasulu, N. (2019). Long glucan
855 chains reduce in vitro starch digestibility of freshly cooked and retrograded
856 milled rice. *Journal of Cereal Science, 86,* 108-116.
857 https://doi.org/10.1016/j.jcs.2019.02.001

858 Amoako, D. B., & Awika, J. M. (2019). Resistant starch formation through
859 intrahelical V-complexes between polymeric proanthocyanidins and amylose.
860 *Food Chemistry, 285*, 326-333. https://doi.org/10.1016/j.foodchem.2019.01.173

861 Beaucage, G. (1995). Approximations leading to a unified exponential/power-law
862 approach to small-angle scattering. *Journal of Applied Crystallography, 28,*
863 717-728. https://doi.org/10.1107/S0021889895005292

864 Bertoft, E. (2017). Understanding Starch Structure: Recent Progress. *Agronomy, 7*, 56.
865 https://doi.org/10.3390/agronomy7030056

866 Bindels, L. B., Walter, J., & Ramer-Tait, A. E. (2015). Resistant starches for the
867 management of metabolic diseases. *Current Opinion in Clinical Nutrition and*
868 *Metabolic Care, 18*, 559. https://doi.org/10.1097/MCO.0000000000000223

869 Blazek, J., & Gilbert, E. P. (2011). Application of small-angle X-ray and neutron
870 scattering techniques to the characterisation of starch structure: A review.
871 *Carbohydrate Polymers, 85,* 281-293.

https://doi.org/10.1016/j.carbpol.2011.02.041

Brennan, C. S. (2005). Dietary fibre, glycaemic response, and diabetes. *Molecular Nutrition & Food Research, 49*, 560-570. https://doi.org/10.1002/mnfr.200500025

Cai, J., Man, J., Huang, J., Liu, Q., Wei, W., & Wei, C. (2015). Relationship between structure and functional properties of normal rice starches with different amylose contents. *Carbohydrate Polymers, 125*, 35-44. https://doi.org/10.1016/j.carbpol.2015.02.067

Cameron, R. E., & Donald, A. M. (1993a). A small-angle X-ray scattering study of the absorption of water into the starch granule. *Carbohydrate Research, 244*, 225-236. https://doi.org/10.1016/0008-6215(83)85003-4

Cameron, R. E., & Donald, A. M. (1993b). A small-angle X-ray scattering study of starch gelatinization in excess and limiting water. *Journal of Polymer Science Part B: Polymer Physics, 31*, 1197-1203. https://doi.org/10.1002/polb.1993.090310914

Carolie, G., Jean, P. A., Guy, M. M., Christian, C., & Françoise, P. (1996). Crystal structure of pig pancreatic alpha-amylase isoenzyme II, in complex with the carbohydrate inhibitor acarbose. *European Journal of Biochemistry, 238*, 561-569. https://doi.org/10.1111/j.1432-1033.1996.0561z.x

892 Castro, J. V. , Dumas C., & H., C. (2005). Mechanistic information from analysis of
893 molecular weight distributions of starch. *Biomacromolecules, 6*, 2248-2259.
894 https://doi.org/10.1021/bm0500401
895 Castro, J.V., R. M. Ward, & Gilbert, R. G. (2005). Measurement of the molecular
896 weight Distribution of debranched starch. *Biomacromolecules, 6*, 2260-2270.
897 https://doi.org/10.1021/bm050041t
898 Chen, B., Guo, Z., Miao, S., Zeng, S., Jia, X., Zhang, Y., & Zheng, B. (2018).
899 Preparation and characterization of lotus seed starch-fatty acid complexes
900 formed by microfluidization. *Journal of Food Engineering, 237*, 52-59.
901 https://doi.org/10.1016/j.jfoodeng.2018.05.020
902 Chen, J. F., Guo, J., Zhang, T., Wan, Z. L., Yang, J., & Yang, X. Q. (2018). Slowing
903 the starch digestion by structural modification through preparing zein/pectin
904 particle stabilized water-in-water emulsion. *Journal of Agricultural and Food*
905 *Chemistry*. https://doi.org/10.1021/acs.jafc.7b05501
906 Chen, L., Zhang, H., McClements, D. J., Zhang, Z., Zhang, R., Jin, Z., & Tian, Y.
907 (2019). Effect of dietary fibers on the structure and digestibility of fried potato
908 starch: A comparison of pullulan and pectin. *Carbohydrate Polymers, 215*, 47-57.
909 https://doi.org/10.1016/j.carbpol.2019.03.046
910 Chen, S. H., Li, X. F., Shih, P. T., & Pai, S. M. (2020). Preparation of thermally stable
911 and digestive enzyme resistant flour directly from Japonica broken rice by

912 combination of steam infusion, enzymatic debranching and heat moisture
913 treatment. *Food Hydrocolloids, 108*.
914 https://doi.org/10.1016/j.foodhyd.2020.106022
915 Chen, Y., Yang, Q., Xu, X., Qi, L., Dong, Z., Luo, Z., Lu, X., & Peng, X. (2017).
916 Structure changes of waxy and normal maize starches modified by heat moisture
917 treatment and their relationship with starch digestibility. *Carbohydrate Polymers,*
918 *177*, 232-240. https://doi.org/10.1016/j.carbpol.2017.08.121
919 Chen, Y., Zhao, L., He, T., Ou, Z., Hu, Z., & Wang, K. (2019). Effects of mango peel
920 powder on starch digestion and quality characteristics of bread. *International*
921 *Journal of Biological Macromolecules, 140*, 647-652.
922 https://doi.org/10.1016/j.ijbiomac.2019.08.188
923 Chi, C., Li, X., Feng, T., Zeng, X., Chen, L., & Li, L. (2018a). Improvement in
924 nutritional attributes of rice starch with dodecyl gallate complexation: a
925 molecular dynamic simulation and *in vitro* study. *Journal of Agricultural and*
926 *Food Chemistry, 66*, 9282-9290. https://doi.org/10.1021/acs.jafc.8b02121
927 Chi, C., Li, X., Lu, P., Miao, S., Zhang, Y., & Chen, L. (2019a). Dry heating and
928 annealing treatment synergistically modulate starch structure and digestibility.
929 *International Journal of Biological Macromolecules, 137*, 554-561.
930 https://doi.org/10.1016/j.ijbiomac.2019.06.137
931 Chi, C., Li, X., Zhang, Y., Chen, L., & Li, L. (2018b). Understanding the mechanism

of starch digestion mitigation by rice protein and its enzymatic hydrolysates. *Food Hydrocolloids, 84*, 473-480. https://doi.org/10.1016/j.foodhyd.2018.06.040

Chi, C., Li, X., Zhang, Y., Chen, L., Li, L., & Wang, Z. (2017). Digestibility and supramolecular structural changes of maize starch by non-covalent interactions with gallic acid. *Food & Function, 8*, 720-730. https://doi.org/10.1039/c6fo01468b

Chi, C., Li, X., Zhang, Y., Chen, L., Xie, F., Li, L., & Bai, G. (2019b). Modulating the in vitro digestibility and predicted glycemic index of rice starch gels by complexation with gallic acid. *Food Hydrocolloids, 89*, 821-828. https://doi.org/10.1016/j.foodhyd.2018.11.016

Chi, C., Li, X., Zhang, Y., Miao, S., Chen, L., Li, L., & Liang, Y. (2020). Understanding the effect of freeze-drying on microstructures of starch hydrogels. *Food Hydrocolloids, 101*. https://doi.org/10.1016/j.foodhyd.2019.105509

Chung, H. J., Liu, Q., Lee, L., & Wei, D. Z. (2011). Relationship between the structure, physicochemical properties and in vitro digestibility of rice starches with different amylose contents. *Food Hydrocolloids, 25*, 968-975. https://doi.org/10.1016/j.foodhyd.2010.09.011

Contardo, I., James, B., & Bouchon, P. (2020). Microstructural characterization of vacuum-fried matrices and their influence on starch digestion. *Food Structure, 25*. https://doi.org/10.1016/j.foostr.2020.100146

952 Dhital, S., Shrestha, A. K., & Gidley, M. J. (2010). Relationship between granule size
953 and in vitro digestibility of maize and potato starches. *Carbohydrate Polymers, 82*, 480-488. https://doi.org/10.1016/j.carbpol.2010.05.018
955 Dhital, S., Shrestha, A. K., Hasjim, J., & Gidley, M. J. (2011). Physicochemical and
956 structural properties of maize and potato starches as a function of granule size.
957 *Journal of Agricultural and Food Chemistry, 59*, 10151-10161.
958 https://doi.org/10.1021/jf202293s
959 Dhital, S., Warren, F. J., Butterworth, P. J., Ellis, P. R., & Gidley, M. J. (2015).
960 Mechanisms of starch digestion by α-amylase—Structural basis for kinetic
961 properties. *Critical Reviews in Food Science and Nutrition, 57*, 875-892.
962 https://doi.org/10.1080/10408398.2014.922043
963 Duan, Y., Wang, Y., Liu, Q., Dong, H., Li, H., Xiong, D., & Zhang, J. (2019). Changes
964 in the intestine microbial, digestion and immunity of Litopenaeus vannamei in
965 response to dietary resistant starch. *Scientific Reports, 9*, 6464.
966 https://doi.org/10.1038/s41598-019-42939-8
967 Dupuis, J. H., Liu, Q., & Yada, R. Y. (2014). Methodologies for increasing the
968 resistant starch content of food starches: A review. *Comprehensive Reviews in*
969 *Food Science and Food Safety, 13*, 1219-1234.
970 https://doi.org/10.1111/1541-4337.12104
971 Englyst, H. N., Kingman, S., & Cummings, J. (1992). Classification and measurement

of nutritionally important starch fractions. *European Journal of Clinical Nutrition, 46*, S33-50.

Fan, D., Wang, L., Chen, W., Ma, S., Ma, W., Liu, X., Zhao, J., & Zhang, H. (2014). Effect of microwave on lamellar parameters of rice starch through small-angle X-ray scattering. *Food Hydrocolloids, 35*, 620-626. https://doi.org/10.1016/j.foodhyd.2013.08.003

Fredriksson, H., Silverio, J., Andersson, R., Eliasson, A. C., & Åman, P. (1998). The influence of amylose and amylopectin characteristics on gelatinization and retrogradation properties of different starches. *Carbohydrate Polymers, 35*, 119-134. https://doi.org/10.1016/S0144-8617(97)00247-6

Freitas, D., Le Feunteun, S., Panouille, M., & Souchon, I. (2018). The important role of salivary alpha-amylase in the gastric digestion of wheat bread starch. *Food & Function, 9*, 200-208. https://doi.org/10.1039/c7fo01484h

Gallant, D. J., Bouchet, B., & Baldwin, P. M. (1997). Microscopy of starch: evidence of a new level of granule organization. *Carbohydrate Polymers, 32*, 177-191. https://doi.org/10.1016/S0144-8617(97)00008-8

Gao, J., Tan, E. Y. N., Low, S. H. L., Wang, Y., Ying, J., Dong, Z., & Zhou, W. (2021). From bolus to digesta: How structural disintegration affects starch hydrolysis during oral-gastro-intestinal digestion of bread. *Journal of Food Engineering, 289*. https://doi.org/10.1016/j.jfoodeng.2020.110161

992 Genyi Zhang, Maghaydah Sofyan, & Hamaker, B. R. (2008). Slowly digestible state
993 of starch: mechanism of slow digestion property of gelatinized maize starch.
994 *Journal of Agricultural and Food Chemistry, 56*, 4695-4702.
995 https://doi.org/10.1021/jf072823e
996 Gidley, M., & Bulpin, P. (1987). Crystallisation of malto-oligosaccharides as models
997 of the crystalline forms of starch: minimum chain-length requirement for the
998 formation of double helices. *Carbohydrate Research, 161*, 291-300.
999 https://doi.org/10.1016/S0008-6215(00)90086-7
1000 Gong, Cheng, Gilbert, & Li. (2019). Distribution of short to medium amylose chains
1001 are major controllers of in vitro digestion of retrograded rice starch. *Food*
1002 *Hydrocolloids, 96*, 634-643. https://doi.org/10.1016/j.foodhyd.2019.06.003
1003 Guo, P., Li, Y., An, J., Shen, S., & Dou, H. (2019). Study on structure-function of
1004 starch by asymmetrical flow field-flow fractionation coupled with multiple
1005 detectors: A review. *Carbohydrate Polymers, 226*, 115330.
1006 https://doi.org/10.1016/j.carbpol.2019.115330
1007 Guo, Z., Jia, X., Lin, X., Chen, B., Sun, S., & Zheng, B. (2019). Insight into the
1008 formation, structure and digestibility of lotus seed amylose-fatty acid complexes
1009 prepared by high hydrostatic pressure. *Food and Chemical Toxicology, 128*,
1010 81-88. https://doi.org/10.1016/j.fct.2019.03.052
1011 Hasjim, J., Lavau, G. C., Gidley, M. J., & Gilbert, R. G. (2010). In vivo and In vitro

1012 starch digestion: Are current in vitro techniques adequate?. *Biomacromolecules, 11*, 3600-3608. https://doi.org/10.1021/bm101053y

1014 He, H., Chi, C., Xie, F., Li, X., Liang, Y., & Chen, L. (2020a). Improving the in vitro 1015 digestibility of rice starch by thermomechanically assisted complexation with 1016 guar gum. *Food Hydrocolloids, 102*, 105637. 1017 https://doi.org/10.1016/j.foodhyd.2019.105637

1018 He, H., Zheng, B., Wang, H., Li, X., & Chen, L. (2020b). Insights into the multi-scale 1019 structure and in vitro digestibility changes of rice starch-oleic acid/linoleic acid 1020 complex induced by heat-moisture treatment. *Food Research International, 137*. 1021 https://doi.org/10.1016/j.foodres.2020.109612

1022 Hong, Y., Liu, G., Zhou, S., Gu, Z., Cheng, L., Li, Z., & Li, C. (2016). Influence of 1023 guar gum on the in vitro digestibility of tapioca starch. *Starch-Stärke, 68*, 1024 339-347. https://doi.org/10.1002/star.201500142

1025 Huang, J., Wei, M., Ren, R., Li, H., Liu, S., & Yang, D. (2017). Morphological 1026 changes of blocklets during the gelatinization process of tapioca starch. 1027 *Carbohydrate Polymers, 163*, 324-329. 1028 https://doi.org/10.1016/j.carbpol.2017.01.083

1029 Huang, J., Wei, N., Li, H., Liu, S., & Yang, D. (2014). Outer shell, inner blocklets, 1030 and granule architecture of potato starch. *Carbohydrate Polymers, 103*, 355-358. 1031 https://doi.org/10.1016/j.carbpol.2013.12.064

1032 Huo, Y., Zhang, B., Niu, M., Jia, C., Zhao, S., Huang, Q., & Du, H. (2018). An insight
1033 into the multi-scale structures and pasting behaviors of starch following citric
1034 acid treatment. *International Journal of Biological Macromolecules, 116*,
1035 793-800. https://doi.org/10.1016/j.ijbiomac.2018.05.114
1036 Hurd, A. J., & Flower, W. L. (1988). In situ growth and structure of fractal silica
1037 aggregates in a flame. *Journal of Colloid and Interface Science*, *122*, 178-192.
1038 https://doi.org/10.1016/0021-9797(88)90301-3
1039 Jane, J. L., Wong, K. S., & McPherson, A. E. (1997). Branch-structure difference in
1040 starches of A- and B-type x-ray patterns revealed by their Naegeli dextrins.
1041 *Carbohydrate Research*, *300*, 219-227.
1042 https://doi.org/10.1016/s0008-6215(97)00056-6
1043 Kim, B. S., Kim, H.-S., Hong, J. S., Huber, K. C., Shim, J. H., & Yoo, S.-H. (2013).
1044 Effects of amylosucrase treatment on molecular structure and digestion
1045 resistance of pre-gelatinised rice and barley starches. *Food Chemistry, 138*,
1046 966-975. https://doi.org/10.1016/j.foodchem.2012.11.028
1047 Kim, B. K., Kim, H. I., Moon, T. W., & Choi, S. J. (2014). Branch chain elongation by
1048 amylosucrase: production of waxy corn starch with a slow digestion property.
1049 *Food Chemistry, 152*, 113-120. https://doi.org/10.1016/j.foodchem.2013.11.145
1050 Kim, B. S., Kim, H. S., Hong, J. S., Huber, K. C., Shim, J. H., & Yoo, S. H. (2013).
1051 Effects of amylosucrase treatment on molecular structure and digestion

1052 resistance of pre-gelatinised rice and barley starches. *Food Chemistry, 138*,
1053 966-975. https://doi.org/10.1016/j.foodchem.2012.11.028
1054 Kim, H. S., & Huber, K. C. (2008). Channels within soft wheat starch A- and B-type
1055 granules. *Journal of Cereal Science, 48*, 159-172.
1056 https://doi.org/10.1016/j.jcs.2007.09.002
1057 Kim, H. R., Choi, S. J., Choi, H. D., Park, C. S., & Moon, T. W. (2020).
1058 Amylosucrase-modified waxy potato starches recrystallized with amylose: The
1059 role of amylopectin chain length in formation of low-digestible fractions. *Food*
1060 *Chemistry, 318*, 126490. https://doi.org/10.1016/j.foodchem.2020.126490
1061 Kim, H. R., Choi, S. J., Park, C. S., & Moon, T. W. (2017). Kinetic studies of in vitro
1062 digestion of amylosucrase-modified waxy corn starches based on branch chain
1063 length distributions. *Food Hydrocolloids, 65*, 46-56.
1064 https://doi.org/10.1016/j.foodhyd.2016.10.038
1065 Kim, J. H., Kim, H. R., Choi, S. J., Park, C. S., & Moon, T. W. (2016). Production of
1066 an in vitro low-digestible starch via hydrothermal treatment of
1067 amylosucrase-modified normal and waxy rice starches and its structural
1068 properties. *Journal of Agricultural and Food Chemistry, 64*, 5045-5052.
1069 https://doi.org/10.1021/acs.jafc.6b01055
1070 Kuang, Q., Xu, J., Liang, Y., Xie, F., Tian, F., Zhou, S., & Liu, X. (2017). Lamellar
1071 structure change of waxy corn starch during gelatinization by time-resolved

synchrotron SAXS. *Food Hydrocolloids, 62*, 43-48. https://doi.org/10.1016/j.foodhyd.2016.07.024

Lehmann, U., & Robin, F. (2007). Slowly digestible starch – its structure and health implications: a review. *Trends in Food Science & Technology, 18*, 346-355. https://doi.org/10.1016/j.tifs.2007.02.009

Li, C., Gong, B., Hu, Y., Liu, X., Guan, X., & Zhang, B. (2020). Combined crystalline, lamellar and granular structural insights into in vitro digestion rate of native starches. *Food Hydrocolloids, 105*. https://doi.org/10.1016/j.foodhyd.2020.105823

Li, C., Hu, Y., Tao, H., Gong, B., & Yu, W. W. (2020). A combined action of amylose and amylopectin fine molecular structures in determining the starch pasting and retrogradation property. *International Journal of Biological Macromolecules*. https://doi.org/10.1016/j.ijbiomac.2020.08.123

Li, G., & Zhu, F. (2017). Amylopectin molecular structure in relation to physicochemical properties of quinoa starch. *Carbohydrate Polymers, 164*, 396-402. https://doi.org/10.1016/j.carbpol.2017.02.014

Li, H., Gidley, M. J., & Dhital, S. (2019). High-amylose starches to bridge the “fiber gap”: Development, structure, and nutritional functionality. *Comprehensive Reviews in Food Science and Food Safety, 18*, 362-379. https://doi.org/10.1111/1541-4337.12416

1092 Li, M. N., Zhang, B., Xie, Y., & Chen, H. Q. (2019). Effects of debranching and
1093 repeated heat-moisture treatments on structure, physicochemical properties and
1094 in vitro digestibility of wheat starch. *Food Chemistry, 294*, 440-447.
1095 https://doi.org/10.1016/j.foodchem.2019.05.040
1096 Li, N., Cai, Z., Guo, Y., Xu, T., Qiao, D., Zhang, B., Zhao, S., Huang, Q., Niu, M., Jia,
1097 C., Lin, L., & Lin, Q. (2019). Hierarchical structure and slowly digestible
1098 features of rice starch following microwave cooking with storage. *Food*
1099 *Chemistry, 295*, 475-483. https://doi.org/10.1016/j.foodchem.2019.05.151
1100 Li, Q., Wu, Q. Y., Jiang, W., Qian, J. Y., Zhang, L., Wu, M., Rao, S. Q., & Wu, C. S.
1101 (2019). Effect of pulsed electric field on structural properties and digestibility of
1102 starches with different crystalline type in solid state. *Carbohydrate Polymers, 207*, 362-370. https://doi.org/10.1016/j.carbpol.2018.12.001
1104 Li, W., Zhang, W., Gong, S., Gu, X., Yu, Y., Wu, J., & Wang, Z. (2020). Low and high
1105 methoxyl pectin lowers on structural change and digestibility of fried potato
1106 starch. *LWT - Food Science and Technology, 132*.
1107 https://doi.org/10.1016/j.lwt.2020.109853
1108 Li, Y., Ren, J., Liu, J., Sun, L., Wang, Y., Liu, B., Li, C., & Li, Z. (2018). Modification
1109 by alpha-d-glucan branching enzyme lowers the in vitro digestibility of starch
1110 from different sources. *International Journal of Biological Macromolecules, 107*,
1111 1758-1764. https://doi.org/10.1016/j.ijbiomac.2017.10.049

1112 Lin, L., Chi, C., & Wu, C. (2019). How to calculate starch lamellar features with
1113 improved accuracy by small angle X-ray scattering. *International Journal of*
1114 *Biological Macromolecules, 141*, 622-625.
1115 https://doi.org/10.1016/j.ijbiomac.2019.09.054
1116 Lin, L., Guo, D., Huang, J., Zhang, X., Zhang, L., & Wei, C. (2016). Molecular
1117 structure and enzymatic hydrolysis properties of starches from high-amylose
1118 maize inbred lines and their hybrids. *Food Hydrocolloids, 58*, 246-254.
1119 https://doi.org/10.1016/j.foodhyd.2016.03.001
1120 Lin, L., Zhang, L., Cai, X., Liu, Q., Zhang, C., & Wei, C. (2018). The relationship
1121 between enzyme hydrolysis and the components of rice starches with the same
1122 genetic background and amylopectin structure but different amylose contents.
1123 *Food Hydrocolloids, 84*, 406-413. https://doi.org/10.1016/j.foodhyd.2018.06.029
1124 Lin, L., Zhang, Q., Zhang, L., & Wei, C. (2017). Evaluation of the molecular
1125 structural parameters of normal rice starch and their relationships with its
1126 thermal and digestion properties. *Molecules, 22*, 1526.
1127 https://doi.org/10.3390/molecules22091526
1128 Liu, H., Yu, L., Xie, F., & Chen, L. (2006). Gelatinization of cornstarch with different
1129 amylose/amylopectin content. *Carbohydrate Polymers, 65*, 357-363.
1130 https://doi.org/10.1016/j.carbpol.2006.01.026
1131 Liu, K., Zhang, B., Chen, L., Li, X., & Zheng, B. (2019). Hierarchical structure and

physicochemical properties of highland barley starch following heat moisture treatment. *Food Chemistry, 271*, 102-108. https://doi.org/10.1016/j.foodchem.2018.07.193

Liu, K., Zu, Y., Chi, C., Gu, B., Chen, L., & Li, X. (2018). Modulation of the digestibility and multi-scale structure of cassava starch by controlling the cassava growth period. *International Journal of Biological Macromolecules, 120*, 346-353. https://doi.org/10.1016/j.ijbiomac.2018.07.184

Liu, W., Hong, Y., Gu, Z., Cheng, L., Li, Z., & Li, C. (2017). In structure and in - vitro digestibility of waxy corn starch debranched by pullulanase. *Food Hydrocolloids, 67*, 104-110. https://doi.org/10.1016/j.foodhyd.2016.12.036

Liu, Y., Chen, L., Xu, H., Liang, Y., & Zheng, B. (2019). Understanding the digestibility of rice starch-gallic acid complexes formed by high pressure homogenization. *International Journal of Biological Macromolecules, 134*, 856-863. https://doi.org/10.1016/j.ijbiomac.2019.05.083

Lu, Z. H., Donner, E., Yada, R. Y., & Liu, Q. (2016). Physicochemical properties and in vitro starch digestibility of potato starch/protein blends. *Carbohydrate Polymers, 154*, 214-222. https://doi.org/10.1016/j.carbpol.2016.08.055

Ludwig, D. S., Hu, F. B., Tappy, L., & Brand-Miller, J. (2018). Dietary carbohydrates: role of quality and quantity in chronic disease. *BMJ, 361*, k2340. https://doi.org/10.1136/bmj.k2340

1152 Magallanes, C. P. A., Flores, S. P. C., & Bello, P. L. A. (2017). Starch Structure
1153 Influences Its Digestibility: A Review. *Journal of Food Science, 82*, 2016-2023.
1154 https://doi.org/10.1111/1750-3841.13809
1155 Martinez, M. M., Li, C., Okoniewska, M., Mukherjee, I., Vellucci, D., & Hamaker, B.
1156 (2018). Slowly digestible starch in fully gelatinized material is structurally
1157 driven by molecular size and A and B1 chain lengths. *Carbohydrate Polymers, 197*, 531-539. https://doi.org/10.1016/j.carbpol.2018.06.021
1159 Miao, M., Jiang, B., Cui, S. W., Zhang, T., & Jin, Z. (2015a). Slowly digestible
1160 starch--a review. *Critical Reviews in Food Science and Nutrition, 55*, 1642-1657.
1161 https://doi.org/10.1080/10408398.2012.704434
1162 Miao, M., Jiang, B., & Zhang, T. (2009). Effect of pullulanase debranching and
1163 recrystallization on structure and digestibility of waxy maize starch.
1164 *Carbohydrate Polymers, 76*, 214-221.
1165 https://doi.org/10.1016/j.carbpol.2008.10.007
1166 Miao, M., Li, R., Huang, C., Jiang, B., & Zhang, T. (2015b). Impact of beta-amylase
1167 degradation on properties of sugary maize soluble starch particles. *Food*
1168 *Chemistry, 177*, 1-7. https://doi.org/10.1016/j.foodchem.2014.12.101
1169 Miao, M., Xiong, S., Jiang, B., Jiang, H., Cui, S. W., & Zhang, T. (2014a).
1170 Dual-enzymatic modification of maize starch for increasing slow digestion
1171 property. *Food Hydrocolloids, 38*, 180-185.

https://doi.org/10.1016/j.foodhyd.2013.12.006

Miao, M., Xiong, S., Jiang, B., Jiang, H., Cui, S. W., & Zhang, T. (2014). Improved the slow digestion property of maize starch using partially beta-amylolysis. *Food Chemistry, 152*, 128-132. https://doi.org/10.1016/j.foodchem.2013.11.148

Miao, M., Xiong, S., Jiang, B., Jiang, H., Cui, S. W., & Zhang, T. (2014b). Improved the slow digestion property of maize starch using partially β-amylolysis. *Food Chemistry, 152*, 128-132. https://doi.org/10.1016/j.foodchem.2013.11.148

Miao, M., Xiong, S., Ye, F., Jiang, B., Cui, S. W., & Zhang, T. (2014c). Development of maize starch with a slow digestion property using maltogenic α-amylase. *Carbohydrate Polymers, 103*, 164-169. https://doi.org/10.1016/j.carbpol.2013.12.041

Miao, M., Zhang, T., Mu, W., & Jiang, B. (2010). Effect of controlled gelatinization in excess water on digestibility of waxy maize starch. *Food Chemistry, 119*, 41-48. https://doi.org/10.1016/j.foodchem.2009.05.035

Benmoussa, M., Moldenhauer K. A. K., & Hamaker, B. R. (2007). Rice amylopectin fine structure variability affects starch digestion properties. *Journal of Agricultural and Food Chemistry, 55*, 1475-1479. https://doi.org/10.1021/jf062349x

Nada, S. S., Zou, W., Li, C., & Gilbert, R. G. (2017). Parameterizing amylose chain-length distributions for biosynthesis-structure-property relations. *Anal*

Bioanal Chem, 409, 6813-6819. https://doi.org/10.1007/s00216-017-0639-5

Pikus, S. (2005). Small-angle X-ray scattering (SAXS) studies of the structure of starch and starch products. *Fibres and Textiles in Eastern Europe, 13,* 82-86.

Pu, H., Chen, L., Li, L., & Li, X. (2013). Multi-scale structural and digestion resistibility changes of high-amylose corn starch after hydrothermal-pressure treatment at different gelatinizing temperatures. *Food Research International, 53,* 456-463. https://doi.org/10.1016/j.foodres.2013.05.021

Qiao, D., Tu, W., Liao, A., Li, N., Zhang, B., Jiang, F., Zhong, L., Zhao, S., Zhang, L., & Lin, Q. (2019). Multi-scale structure and pasting/digestion features of yam bean tuber starches. *Carbohydrate Polymers, 213,* 199-207. https://doi.org/10.1016/j.carbpol.2019.02.082

Qiao, D., Tu, W., Zhang, B., Wang, R., Li, N., Nishinari, K., Riffat, S., & Jiang, F. (2019). Understanding the multi-scale structure and digestion rate of water chestnut starch. *Food Hydrocolloids, 91,* 311-318. https://doi.org/10.1016/j.foodhyd.2019.01.036

Qiao, D., Xie, F., Zhang, B., Zou, W., Zhao, S., Niu, M., Lv, R., Cheng, Q., Jiang, F., & Zhu, J. (2016). A further understanding of the multi-scale supramolecular structure and digestion rate of waxy starch. *Food Hydrocolloids*. https://doi.org/10.1016/j.foodhyd.2016.10.041

Qiao, D., Yu, L., Liu, H., Zou, W., Xie, F., Simon, G., Petinakis, E., Shen, Z., & Chen,

L. (2016). Insights into the hierarchical structure and digestion rate of alkali-modulated starches with different amylose contents. *Carbohydrate Polymers, 144*, 271-281. https://doi.org/10.1016/j.carbpol.2016.02.064

Raigond, P., Ezekiel, R., & Raigond, B. (2015). Resistant starch in food: A review. *Journal of the Science of Food and Agriculture, 95*, 1968-1978. https://doi.org/10.1002/jsfa.6966

Rashmi, S., & Urooj, A. (2003). Effect of processing on nutritionally important starch fractions in rice varieties. *International journal of food sciences and nutrition, 54*, 27-36. https://doi.org/10.1080/096374803161976

Rehman, A., Heinsen, F.-A., Koenen, M. E., Venema, K., Knecht, H., Hellmig, S., Schreiber, S., & Ott, S. J. (2012). Effects of probiotics and antibiotics on the intestinal homeostasis in a computer controlled model of the large intestine. *BMC Microbiology, 12*, 47. http://www.biomedcentral.com/1471-2180/12/47

Robyt, J. F. (2009). Enzymes and their action on starch. In *Studia archaeologica* (pp. 237-292): Elsevier. https://doi.org/10.1016/B978-0-12-746275-2.00007-0

Rovalino-Córdova, A. M., Fogliano, V., & Capuano, E. (2018). A closer look to cell structural barriers affecting starch digestibility in beans. *Carbohydrate Polymers, 181*, 994-1002. https://doi.org/10.1016/j.carbpol.2017.11.050

Selma-Gracia, R., Laparra, J. M., & Haros, C. M. (2020). Potential beneficial effect of hydrothermal treatment of starches from various sources on *in vitro* digestion.

Food Hydrocolloids, 103. https://doi.org/10.1016/j.foodhyd.2020.105687

Shen, X., Bertoft, E., Zhang, G., & Hamaker, B. R. (2013). Iodine binding to explore the conformational state of internal chains of amylopectin. *Carbohydrate Polymers, 98*, 778-783. https://doi.org/10.1016/j.carbpol.2013.06.050

Shi, Y. C., & Seib, P. A. (1992). The structure of four waxy starches related to gelatinization and retrogradation. *Carbohydrate Research, 227*, 131-145. https://doi.org/10.1016/0008-6215(92)85066-9

Situ, W., Chen, L., Wang, X., & Li, X. (2014). Resistant starch film-coated microparticles for an oral colon-specific polypeptide delivery system and its release behaviors. *Journal of Agricultural and Food Chemistry, 62*, 3599-3609. https://doi.org/10.1021/jf500472b

Srichuwong, S., Sunarti, T., Mishima, T., Isono, N., & Hisamatsu, M. (2005). Starches from different botanical sources I: Contribution of amylopectin fine structure to thermal properties and enzyme digestibility. *Carbohydrate Polymers, 60*, 529-538. https://doi.org/10.1016/j.carbpol.2005.03.004

Striegel, A., Yau, W. W., Kirkland, J. J., & Bly, D. D. (2009). *Modern size-exclusion liquid chromatography: practice of gel permeation and gel filtration chromatography*: John Wiley & Sons.

Sun, Y., Wu, H., Dong, W., Zhou, J., Zhang, X., Liu, L., Zhang, X., Cheng, H., Guan, J., Zhao, R., & Mao, S. (2019). Molecular simulation approach to the rational

1252 design of self-assembled nanoparticles for enhanced peroral delivery of
1253 doxorubicin. *Carbohydrate Polymers, 218*, 279-288.
1254 https://doi.org/10.1016/j.carbpol.2019.04.095
1255 Suzuki, T., Chiba, A., & Yano, T. (1997). Interpretation of small angle X-ray
1256 scattering from starch on the basis of fractals. *Carbohydrate Polymers, 34*,
1257 357-363. https://doi.org/10.1016/s0144-8617(97)00170-7
1258 Svihus, B., & Hervik, A. K. (2016). Digestion and metabolic fates of starch, and its
1259 relation to major nutrition-related health problems: A review. *Starch - Stärke, 68*,
1260 302-313. https://doi.org/10.1002/star.201500295
1261 Syahariza, Z., Sar, S., Hasjim, J., Tizzotti, M. J., & Gilbert, R. G. (2013). The
1262 importance of amylose and amylopectin fine structures for starch digestibility in
1263 cooked rice grains. *Food Chemistry, 136*, 742-749.
1264 https://doi.org/10.1016/j.foodchem.2012.08.053
1265 Tan, L., & Kong, L. (2019). Starch-guest inclusion complexes: Formation, structure,
1266 and enzymatic digestion. *Critical Reviews in Food Science and Nutrition*, 1-11.
1267 https://doi.org/10.1080/10408398.2018.1550739
1268 Tan, X., Li, X., Chen, L., Xie, F., Li, L., & Huang, J. (2017). Effect of heat-moisture
1269 treatment on multi-scale structures and physicochemical properties of breadfruit
1270 starch. *Carbohydrate Polymers, 161*, 286-294.
1271 https://doi.org/10.1016/j.carbpol.2017.01.029

1272 Tan, X., Zhang, B., Chen, L., Li, X., Li, L., & Xie, F. (2015). Effect of planetary
1273 ball-milling on multi-scale structures and pasting properties of waxy and
1274 high-amylose cornstarches. *Innovative Food Science & Emerging Technologies, 30*, 198-207. https://doi.org/10.1016/j.ifset.2015.03.013
1276 Tang, H., Mitsunaga, T., & Kawamura, Y. (2006). Molecular arrangement in blocklets
1277 and starch granule architecture. *Carbohydrate Polymers, 63*, 555-560.
1278 https://doi.org/10.1016/j.carbpol.2005.10.016
1279 Tao, K., Li, C., Yu, W., Gilbert, R. G., & Li, E. (2019). How amylose molecular fine
1280 structure of rice starch affects functional properties. *Carbohydrate Polymers, 204*,
1281 24-31. https://doi.org/10.1016/j.carbpol.2018.09.078
1282 Tester, R., Qi, X., & Karkalas, J. (2006). Hydrolysis of native starches with amylases.
1283 *Animal Feed Science and Technology, 130*, 39-54.
1284 https://doi.org/10.1016/j.anifeedsci.2006.01.016
1285 Tian, J., Ogawa, Y., Shi, J., Chen, S., Zhang, H., Liu, D., & Ye, X. (2018). The
1286 microstructure of starchy food modulates its digestibility. *Critical Reviews in*
1287 *Food Science and Nutrition*, 1-51.
1288 https://doi.org/10.1080/10408398.2018.1484341
1289 Toutounji, M. R., Farahnaky, A., Santhakumar, A. B., Oli, P., Butardo, V. M., &
1290 Blanchard, C. L. (2019). Intrinsic and extrinsic factors affecting rice starch
1291 digestibility. *Trends in Food Science & Technology, 88*, 10-22.

https://doi.org/10.1016/j.tifs.2019.02.012

Trung, P. T. B., Ngoc, L. B. B., Hoa, P. N., Tien, N. N. T., & Hung, P. V. (2017). Impact of heat-moisture and annealing treatments on physicochemical properties and digestibility of starches from different colored sweet potato varieties. *International Journal of Biological Macromolecules, 105*, 1071-1078. https://doi.org/10.1016/j.ijbiomac.2017.07.131

Vaclavik, V. A.; Christian, E. W., Essentials of Food Science, Springer: 2014; pp 39-51.

Vamadevan, V., Bertoft, E., & Seetharaman, K. (2013). On the importance of organization of glucan chains on thermal properties of starch. *Carbohydrate Polymers, 92*, 1653-1659. https://doi.org/10.1016/j.carbpol.2012.11.003

Vamadevan, V., Bertoft, E., Soldatov, D. V., & Seetharaman, K. (2013). Impact on molecular organization of amylopectin in starch granules upon annealing. *Carbohydrate Polymers, 98*, 1045-1055. https://doi.org/10.1016/j.carbpol.2013.07.006

Hung, P. V., Chau, H. T., & Phi, N. T. (2016). In vitro digestibility and in vivo glucose response of native and physically modified rice starches varying amylose contents. *Food Chemistry, 191*, 74-80. https://doi.org/10.1016/j.foodchem.2015.02.118

Soest, J. J. V., Tournois, H., de Wit, D., & Vliegenthart, J. F. (1995). Short-range

structure in (partially) crystalline potato starch determined with attenuated total reflectance Fourier-transform IR spectroscopy. *Carbohydrate Research, 279*, 201-214. https://doi.org/10.1016/0008-6215(95)00270-7

Vandeputte, G. E., Vermeylen, R., Geeroms, J., & Delcour, J. A. (2003). Rice starches. III. Structural aspects provide insight in amylopectin retrogradation properties and gel texture. *Journal of Cereal Science, 38*, 61-68. https://doi.org/10.1016/s0733-5210(02)00142-x

Vermeylen, R., Derycke, V., Delcour, J. A., Goderis, B., Reynaers, H., & Koch, M. H. J. (2006). Structural transformations during gelatinization of starches in limited water: combined wide- and small-angle X-ray scattering study. *Biomacromolecules, 7*, 1231-1238. https://doi.org/10.1021/bm050651t

Vilaplana, F., & Gilbert, R. G. (2010). Characterization of branched polysaccharides using multiple-detection size separation techniques. *Journal of Separaton Science, 33*, 3537-3554. https://doi.org/10.1002/jssc.201000525

Wang, H., Liu, Y., Chen, L., Li, X., Wang, J., & Xie, F. (2018). Insights into the multi-scale structure and digestibility of heat-moisture treated rice starch. *Food Chemistry, 242*, 323-329. https://doi.org/10.1016/j.foodchem.2017.09.014

Wang, H., Zhang, B., Chen, L., & Li, X. (2016). Understanding the structure and digestibility of heat-moisture treated starch. *International Journal of Biological Macromolecules, 88*, 1-8. https://doi.org/10.1016/j.ijbiomac.2016.03.046

1332 Wang, K., Vilaplana, F., Wu, A., Hasjim, J., & Gilbert, R. G. (2019). The size
1333 dependence of the average number of branches in amylose. *Carbohydrate*
1334 *Polymers, 223*, 115134. https://doi.org/10.1016/j.carbpol.2019.115134
1335 Wang, L., Zhao, S., Kong, J., Li, N., Qiao, D., Zhang, B., Xu, Y., & Jia, C. (2020).
1336 Changing cooking mode can slow the starch digestion of colored brown rice: A
1337 view of starch structural changes during cooking. *International Journal of*
1338 *Biological Macromolecules, 155*, 226-232.
1339 https://doi.org/10.1016/j.ijbiomac.2020.03.203
1340 Wang, R., Zhang, H., Chen, Z., & Zhong, Q. (2020). Structural basis for the low
1341 digestibility of starches recrystallized from side chains of amylopectin modified
1342 by amylosucrase to different chain lengths. *Carbohydrate Polymers, 241*, 116352.
1343 https://doi.org/10.1016/j.carbpol.2020.116352
1344 Wang, S., Chao, C., Cai, J., Niu, B., Copeland, L., & Wang, S. (2020). Starch–lipid
1345 and starch–lipid–protein complexes: A comprehensive review. *Comprehensive*
1346 *Reviews in Food Science and Food Safety*, 1-24.
1347 https://doi.org/10.1111/1541-4337.12550
1348 Wang, S., & Copeland, L. (2013). Molecular disassembly of starch granules during
1349 gelatinization and its effect on starch digestibility: a review. *Food & Function, 4*,
1350 1564-1580. https://doi.org/10.1039/c3fo60258c
1351 Wang, S., Sun, Y., Wang, J., Wang, S., & Copeland, L. (2016). Molecular disassembly

of rice and lotus starches during thermal processing and its effect on starch digestibility. *Food & Function, 7*, 1188-1195. https://doi.org/10.1039/c6fo00067c

Wang, S., Wang, S., Liu, L., Wang, S., & Copeland, L. (2017). Structural orders of wheat starch do not determine the in vitro enzymatic digestibility. *Journal of Agricultural and Food Chemistry*. https://doi.org/10.1021/acs.jafc.6b04044

Witt, T., Gidley, M. J., & Gilbert, R. G. (2010). Starch digestion mechanistic information from the time evolution of molecular size distributions. *Journal of Agricultural and Food Chemistry, 58*, 8444-8452. https://doi.org/10.1021/jf101063m

Wu, M., He, Q., Hong, Y., & Wang, S. (2016). Preheating of kidney bean proteins enhances cross-linking and functional properties with chicken myofibrillar proteins induced by transglutaminase. *LWT - Food Science and Technology, 65*, 816-822. https://doi.org/10.1016/j.lwt.2015.09.019

Xie, X., Qi, L., Xu, C., Shen, Y., Wang, H., & Zhang, H. (2020). Understanding how the cooking methods affected structures and digestibility of native and heat-moisture treated rice starches. *Journal of Cereal Science, 95*. https://doi.org/10.1016/j.jcs.2020.103085

Xie, Y., Li, M. N., Chen, H. Q., & Zhang, B. (2019). Effects of the combination of repeated heat-moisture treatment and compound enzymes hydrolysis on the

1372 structural and physicochemical properties of porous wheat starch. *Food*
1373 *Chemistry, 274*, 351-359. https://doi.org/10.1016/j.foodchem.2018.09.034
1374 Xu, J., Blennow, A., Li, X., Chen, L., & Liu, X. (2019). Gelatinization dynamics of
1375 starch in dependence of its lamellar structure, crystalline polymorphs and
1376 amylose content. *Carbohydrate Polymers*, 115481.
1377 https://doi.org/10.1016/j.carbpol.2019.115481
1378 Xu, J., Ma, Z., Ren, N., Li, X., Liu, L., & Hu, X. (2019). Understanding the
1379 multi-scale structural changes in starch and its physicochemical properties during
1380 the processing of chickpea, navy bean, and yellow field pea seeds. *Food*
1381 *Chemistry, 289*, 582-590. https://doi.org/10.1016/j.foodchem.2019.03.093
1382 Yan, Y., Feng, L., Shi, M., Cui, C., & Liu, Y. (2020). Effect of plasma-activated water
1383 on the structure and in vitro digestibility of waxy and normal maize starches
1384 during heat-moisture treatment. *Food Chemistry, 306*, 125589.
1385 https://doi.org/10.1016/j.foodchem.2019.125589
1386 Yang, C., Zhong, F., Douglas Goff, H., & Li, Y. (2019). Study on starch-protein
1387 interactions and their effects on physicochemical and digestible properties of the
1388 blends. *Food Chemistry, 280*, 51-58.
1389 https://doi.org/10.1016/j.foodchem.2018.12.028
1390 Yang, X., Chi, C., Liu, X., Zhang, Y., Zhang, H., & Wang, H. (2019). Understanding
1391 the structural and digestion changes of starch in heat-moisture treated polished

1392 rice grains with varying amylose content. *International Journal of Biological*
1393 *Macromolecules, 139,* 785-792. https://doi.org/10.1016/j.ijbiomac.2019.08.051
1394 Yang, Y., Li, T., Li, Y., Qian, H., Qi, X., Zhang, H., & Wang, L. (2020).
1395 Understanding the molecular weight distribution, in vitro digestibility and
1396 rheological properties of the deep-fried wheat starch. *Food Chemistry, 331*,
1397 127315. https://doi.org/10.1016/j.foodchem.2020.127315
1398 Yang, Z., Gu, Q., Lam, E., Tian, F., Chaieb, S., & Hemar, Y. (2016). In situ study
1399 starch gelatinization under ultra-high hydrostatic pressure using synchrotron
1400 SAXS. *Food Hydrocolloids, 56,* 58-61.
1401 https://doi.org/10.1016/j.foodhyd.2015.12.007
1402 Yang, Z., Xu, X., Singh, R., de Campo, L., Gilbert, E. P., Wu, Z., & Hemar, Y. (2019).
1403 Effect of amyloglucosidase hydrolysis on the multi-scale supramolecular
1404 structure of corn starch. *Carbohydrate Polymers, 212,* 40-50.
1405 https://doi.org/10.1016/j.carbpol.2019.02.028
1406 Zu, Y., Zhang B., Chen, L., Xie, F., Li, L., & Li, X. (2016). Supramolecular structural
1407 evolutions of maize starch hydrothermally treated in excess water. *Starch-Stärke,*
1408 *68*, 365-373. https://doi.org/10.1002/star.201500028
1409 Ye, J., Hu, X., Luo, S., McClements, D. J., Liang, L., & Liu, C. (2018). Effect of
1410 endogenous proteins and lipids on starch digestibility in rice flour. *Food*
1411 *Research International, 106,* 404-409.

https://doi.org/10.1016/j.foodres.2018.01.008

Yu, W., Li, H., Zou, W., Tao, K., Zhu, J., & Gilbert, R. G. (2019). Using starch molecular fine structure to understand biosynthesis-structure-property relations. *Trends in Food Science & Technology, 86*, 530-536. https://doi.org/10.1016/j.tifs.2018.08.003

Yu, W., Tao, K., & Gilbert, R. G. (2018). Improved methodology for analyzing relations between starch digestion kinetics and molecular structure. *Food Chemistry, 264*, 284-292. https://doi.org/10.1016/j.foodchem.2018.05.049

Yu, W., Zou, W., Dhital, S., Wu, P., Gidley, M. J., Fox, G. P., & Gilbert, R. G. (2018). The adsorption of α-amylase on barley proteins affects the in vitro digestion of starch in barley flour. *Food Chemistry, 241*, 493-501. https://doi.org/10.1016/j.foodchem.2017.09.021

Zeng, F., Chen, F., Kong, F., Gao, Q., Aadil, R. M., & Yu, S. (2015). Structure and digestibility of debranched and repeatedly crystallized waxy rice starch. *Food Chemistry, 187*, 348-353. https://doi.org/10.1016/j.foodchem.2015.04.033

Zeng, F., Ma, F., Gao, Q., Yu, S., Kong, F., & Zhu, S. (2014). Debranching and temperature-cycled crystallization of waxy rice starch and their digestibility. *Carbohydrate Polymers, 113*, 91-96. https://doi.org/10.1016/j.carbpol.2014.06.057

Zhang, B., Chen, L., Li, X., Li, L., & Zhang, H. (2015). Understanding the multi-scale

structure and functional properties of starch modulated by glow-plasma: A structure-functionality relationship. *Food Hydrocolloids, 50*, 228-236. https://doi.org/10.1016/j.foodhyd.2015.05.002

Zhang, B., Chen, L., Zhao, Y., & Li, X. (2013a). Structure and enzymatic resistivity of debranched high temperature–pressure treated high-amylose corn starch. *Journal of Cereal Science, 57*, 348-355. https://doi.org/10.1016/j.jcs.2012.12.006

Zhang, B., Gilbert, E. P., Qiao, D., Xie, F., Wang, D. K., Zhao, S., & Jiang, F. (2019). A further study on supramolecular structure changes of waxy maize starch subjected to alkaline treatment by extended-q small-angle neutron scattering. *Food Hydrocolloids, 95*, 133-142. https://doi.org/10.1016/j.foodhyd.2019.04.031

Zhang, B., Li, X., Liu, J., Xie, F., & Chen, L. (2013b). Supramolecular structure of A- and B-type granules of wheat starch. *Food Hydrocolloids, 31*, 68-73. https://doi.org/10.1016/j.foodhyd.2012.10.006

Zhang, B., Xie, F., Wang, D. K., Zhao, S., Niu, M., Qiao, D., Xiong, S., Jiang, F., Zhu, J., & Yu, L. (2017). An improved approach for evaluating the semicrystalline lamellae of starch granules by synchrotron SAXS. *Carbohydrate Polymers, 158*, 29-36. https://doi.org/10.1016/j.carbpol.2016.12.002

Zhang, B., Xiong, S., Li, X., Li, L., Xie, F., & Chen, L. (2014a). Effect of oxygen glow plasma on supramolecular and molecular structures of starch and related mechanism. *Food Hydrocolloids, 37*, 69-76.

https://doi.org/10.1016/j.foodhyd.2013.10.034

Zhang, B., Zhao, Y., Li, X., Li, L., Xie, F., & Chen, L. (2014b). Supramolecular structural changes of waxy and high-amylose cornstarches heated in abundant water. *Food Hydrocolloids, 35*, 700-709. https://doi.org/10.1016/j.foodhyd.2013.08.028

Zhang, B., Zhou, W., Qiao, D., Zhang, P., Zhao, S., Zhang, L., & Xie, F. (2019). Changes in nanoscale chain assembly in sweet potato starch lamellae by downregulation of biosynthesis enzymes. *Journal of Agricultural and Food Chemistry, 67*, 6302-6312. https://doi.org/10.1021/acs.jafc.8b06523

Zhang, G., Ao, Z., & Hamaker, B. R. (2008). Nutritional property of endosperm starches from maize mutants: a parabolic relationship between slowly digestible starch and amylopectin fine structure. *Journal of Agricultural and Food Chemistry, 56*, 4686-4694. https://doi.org/10.1021/jf072822m

Zhang, G., & Hamaker, B. R. (2009). Slowly digestible starch: concept, mechanism, and proposed extended glycemic index. *Critical Reviews in Food Science and Nutrition, 49*, 852-867. https://doi.org/10.1080/10408390903372466

Zhang, H., Wang, R., Chen, Z., & Zhong, Q. (2019). Enzymatically modified starch with low digestibility produced from amylopectin by sequential amylosucrase and pullulanase treatments. *Food Hydrocolloids, 95*, 195-202. https://doi.org/10.1016/j.foodhyd.2019.04.036

1472 Zhang, L., Hu, X., Xu, X., Jin, Z., & Tian, Y. (2011). Slowly digestible starch
1473 prepared from rice starches by temperature-cycled retrogradation. *Carbohydrate*
1474 *Polymers, 84*, 970-974. https://doi.org/10.1016/j.carbpol.2010.12.056
1475 Zhang, L., Li, X., Janaswamy, S., Chen, L., & Chi, C. (2020). Further insights into the
1476 evolution of starch assembly during retrogradation using SAXS. *International*
1477 *Journal of Biological Macromolecules, 154*, 521-527.
1478 https://doi.org/10.1016/j.ijbiomac.2020.03.135
1479 Zhang, L., Zhao, Y., Hu, W., Qian, J. Y., Ding, X. L., Guan, C. R., Lu, Y. Q., & Cao, Y.
1480 (2018). Multi-scale structures of cassava and potato starch fractions varying in
1481 granule size. *Carbohydrate Polymers, 200*, 400-407.
1482 https://doi.org/10.1016/j.carbpol.2018.08.022
1483 Zhang, T., Li, X., Chen, L., & Situ, W. (2016). Digestibility and structural changes of
1484 waxy rice starch during the fermentation process for waxy rice vinasse. *Food*
1485 *Hydrocolloids, 57*, 38-45. https://doi.org/10.1016/j.foodhyd.2016.01.004
1486 Zhang, W., Bi, J., Yan, X., Wang, H., Zhu, C., Wang, J., & Wan, J. (2007). In vitro
1487 measurement of resistant starch of cooked milled rice and physico-chemical
1488 characteristics affecting its formation. *Food Chemistry, 105*, 462-468.
1489 https://doi.org/10.1016/j.foodchem.2007.04.002
1490 Zhao, B., Sun, S., Lin, H., Chen, L., Qin, S., Wu, W., Zheng, B., & Guo, Z. (2019a).
1491 Physicochemical properties and digestion of the lotus seed starch-green tea

polyphenol complex under ultrasound-microwave synergistic interaction. *Ultrasonics Sonochemistry, 52*, 50-61. https://doi.org/10.1016/j.ultsonch.2018.11.001

Zhao, B., Wang, B., Zheng, B., Chen, L., & Guo, Z. (2019b). Effects and mechanism of high-pressure homogenization on the characterization and digestion behavior of lotus seed starch–green tea polyphenol complexes. *Journal of Functional Foods, 57*, 173-181. https://doi.org/10.1016/j.jff.2019.04.016

Zheng, M., Su, H., You, Q., Zeng, S., Zheng, B., Zhang, Y., & Zeng, H. (2019). An insight into the retrogradation behaviors and molecular structures of lotus seed starch-hydrocolloid blends. *Food Chemistry, 295*, 548-555. https://doi.org/10.1016/j.foodchem.2019.05.166

Zheng, M., You, Q., Lin, Y., Lan, F., Luo, M., Zeng, H., Zheng, B., & Zhang, Y. (2019). Effect of guar gum on the physicochemical properties and in vitro digestibility of lotus seed starch. *Food Chemistry, 272*, 286-291. https://doi.org/10.1016/j.foodchem.2018.08.029

Zhong, Y., Liu, L., Qu, J., Blennow, A., Hansen, A. R., Wu, Y., Guo, D., & Liu, X. (2020). Amylose content and specific fine structures affect lamellar structure and digestibility of maize starches. *Food Hydrocolloids, 108*. https://doi.org/10.1016/j.foodhyd.2020.105994

Zhu, F. (2018). Relationships between amylopectin internal molecular structure and

physicochemical properties of starch. *Trends in Food Science & Technology, 78,* 234-242. https://doi.org/10.1016/j.tifs.2018.05.024

Figure Captions

Figure 1. The schematic representation of starch hierarchical structures. Amylose and amylopectin are the basic polysaccharides within starch. Amylose binds with hydrophobic guest molecules and forms V-type crystals. Amylopectin associates to form double helices and then arranges into A- or B-type crystals. The orderly-packed A- or B-type crystals and double helices contribute to the formation of lamellar structures that are stacked with amorphous lamellae and crystalline lamellae. Growth rings and blocklets are the semi-crystalline structures with alternating stacks of amorphous and crystalline lamellae.

Figure 2. The schematic representation of the structural changes of starches varying in amylose content during cooking, cooling, and enzymatic digestion.

Figure 3. Schematic starch key structures and their effects on digestibility. The pink arrows indicate the up- or down-regulation of starch structures that mitigate digestibility.

Figure 4 The schematic representation of RDS, SDS, and RS structures. The grey regions indicate starch fractions that are not SDS or RS.

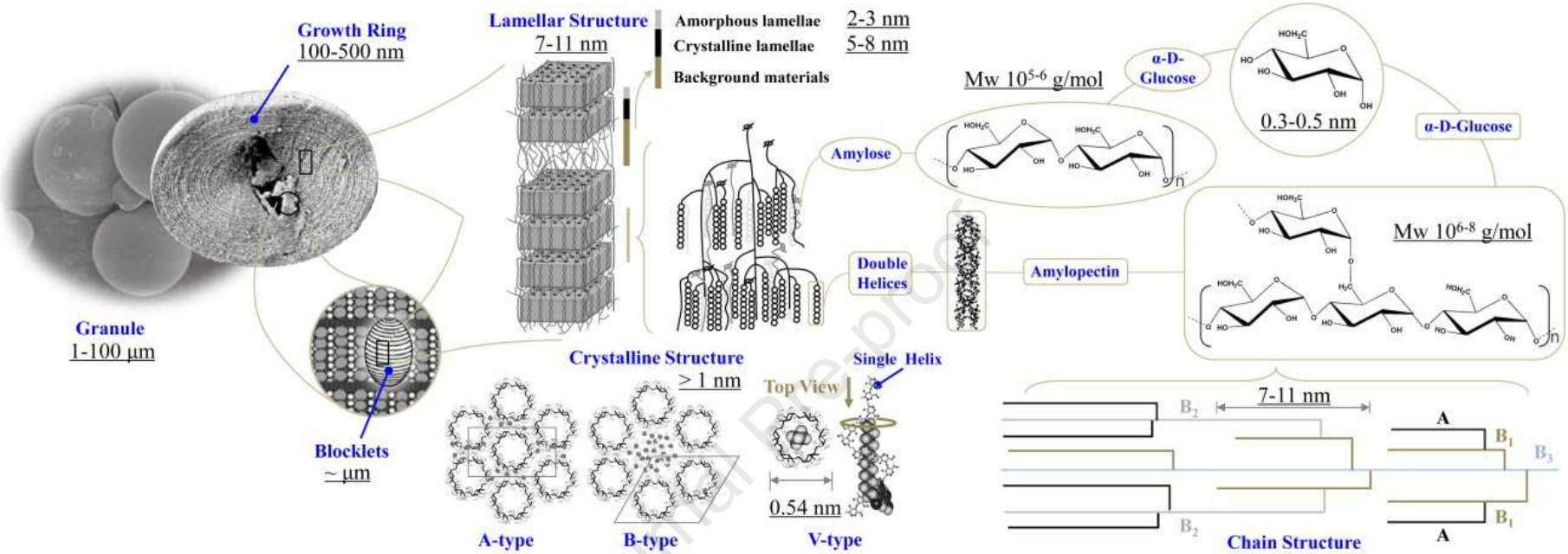
Growth Ring
100-500 nm
Granule
1-100 μm
Blocklets
~ μm
Lamellar Structure
7-11 nm
Amorphous lamellae
Crystalline lamellae
Background materials
2-3 nm
5-8 nm
Amylose
Double Helices
Amylopectin
Mw 10^5-6 g/mol
α-D-Glucose
0.3-0.5 nm
α-D-Glucose
Mw 10^6-8 g/mol
Crystalline Structure
> 1 nm
Single Helix
Top View
0.54 nm
A-type
B-type
V-type
7-11 nm
A
B1
B2
B3
Chain Structure

Figure 1

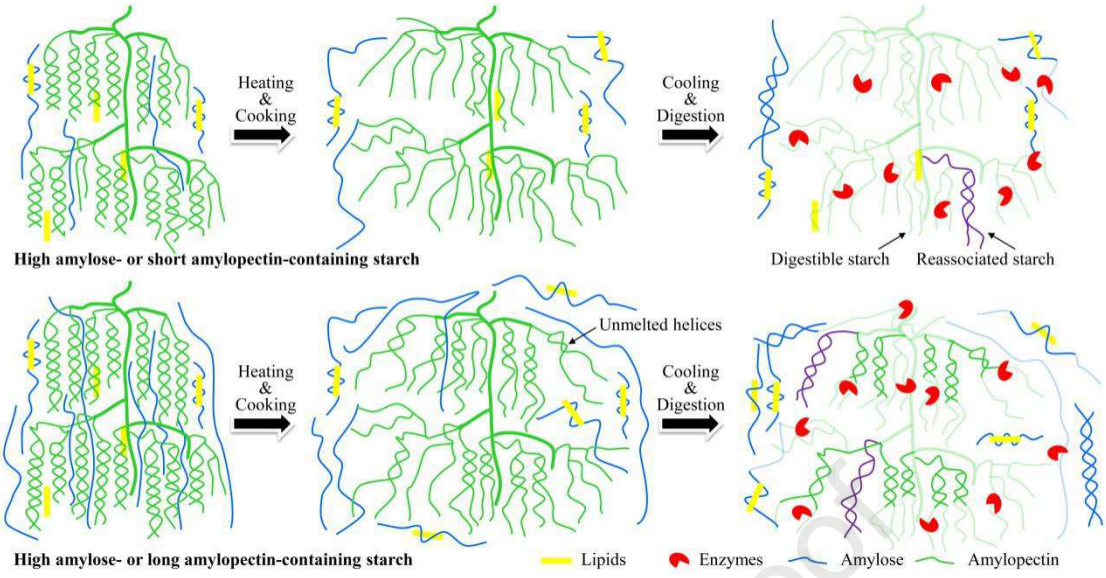

Figure 2

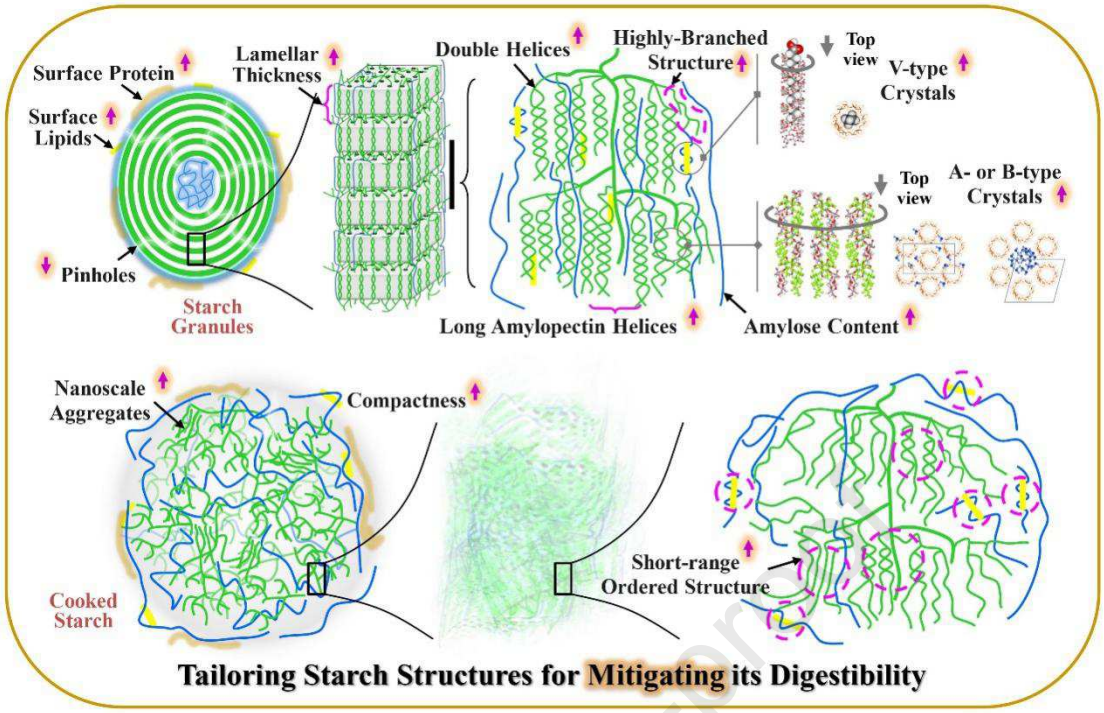

1537

1538 **Figure 3**

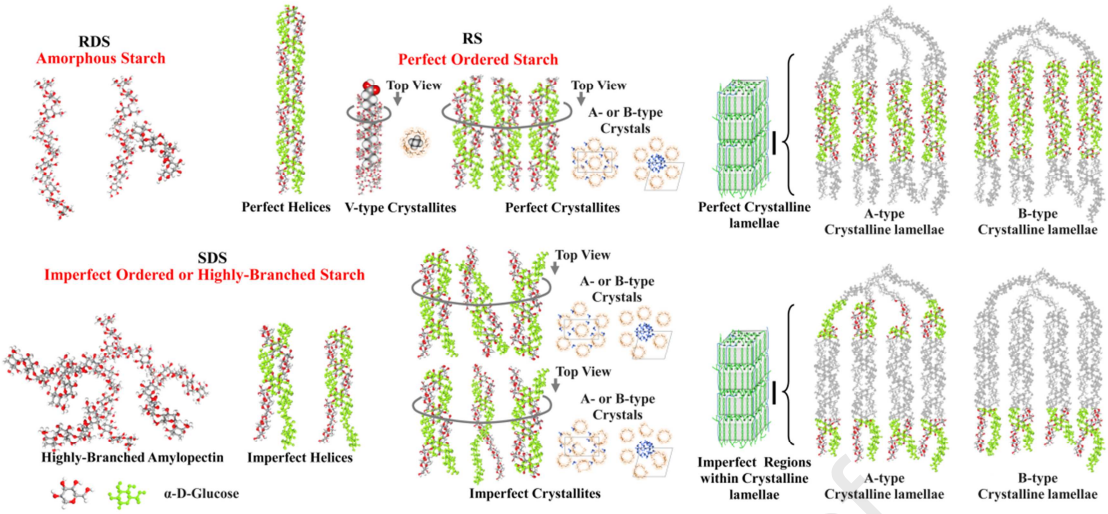

1539

1540 **Figure 4**

1541 **Table 1** Multi-scale structural features of RDS, SDS, and RS.

Structures	RDS	SDS	RS	Reference
Amylose	Low amylose content	High amylose content		Li et al. (2019)
Amylopectin	Random coil (DP < 13) with lower α-1,6 linkages	Short branch chains (DP < 13) with higher α-1,6 linkages and some long chains with DP 25–36	Chains with DP 12–24 and DP ≥ 37 and also some chains with DP 25–36	Kim et al. (2020; Miao et al. (2015b); Miao et al. (2014a, b); Vandeputte et al. (2003); Vermeylen et al. (2006)
Short-range ordered structure	/	Lower ratio and less ordering of short-range ordered structure	Higher ratio and more ordering of short-range ordered structure	Chi et al. (2019a); Chi et al. (2019b); Lu et al. (2020)
Helical structure	/	Imperfectly packed double helices of DP < 13 and DP25–36	V-type single helix, Perfectly packed double helices of DP 12–24 and DP ≥ 37 and also some chains with DP 25–36	Guraya et al. (2001); Kim et al. (2020); Liu et al. (2017); Zhang et al. (2013a)

Crystalline structure	/	Imperfectly packed crystals that are packed by amylopectin with DP < 13 and DP 25–36	V-type crystals, perfectly packed crystals that are packed by amylose, amylopectin with DP 12–24 and DP ≥ 37 and also some chains with DP 25–36	Guraya et al. (2001); Kim et al. (2020); Liu et al. (2017); Zhang et al. (2013a)
Lamellar structure	Amorphous amylose, amorphous amylopectin lamellae	"Weak point"-containing crystalline lamellae, A-type crystalline lamellae	Perfectly packed crystalline lamellae without "weak point"	Jane et al. (1997); Qiao et al. (2019); Qiao et al. (2019); Zhang et al. (2016)
Reassembled aggregate	Amorphous structure	Relatively higher ratio of ordered reassembled aggregate		Chi et al. (2018b); Li et al. (2019); Liu et al. (2019a); Situ et al. (2014)
Fractal structure	Loose structure	Compact structure		He et al. (2020); Liu et al. (2019)

1542

- Reciprocal effects of starch multi-scale structures on starch digestion are reviewed.
- Principles in starch structuration that mitigate starch digestibility are established.
- Perspectives focused on starch structuration and modulation of digestion are presented.
- Multi-scale structural features of starches with differing digestibility are suggested.